

Replicated Functional Evolution in Cichlid Adaptive Radiations

Christopher M. Martinez^{1,*,**}, Katherine A. Corn^{2,3,4, *,**}, Sarah Williamson², Darien Satterfield²,
Alexus S. Roberts-Hugghis², Anthony Barley⁴, Samuel R. Borstein⁶, Matthew D. McGee⁷, and
Peter C. Wainwright²

¹Department of Ecology and Evolutionary Biology, University of California, Irvine, 92697, USA

²Department of Evolution and Ecology, University of California, Davis, 95616, USA

³Department of Biological Sciences, Virginia Polytechnic Institute and State University,
Blacksburg, VA, 24061, USA

⁴School of Biological Sciences, Washington State University, Pullman, WA, 99163, USA

⁵School of Mathematical and Natural Sciences, Arizona State University–West Campus,
Glendale, AZ, 85306, USA

⁶Department of Ecology and Evolutionary Biology, University of Michigan, Ann Arbor, MI,
USA

⁷School of Biological Sciences, Monash University, Melbourne, Victoria, Australia

*Correspondence: c.martinez@uci.edu (C.M.M); cornkatherineap@gmail.com (K.A.C)

**Authors contributed equally to this paper.

ORCIDs: Martinez, <https://orcid.org/0000-0002-3918-1449>; Corn, <https://orcid.org/0000-0002-9437-1683>; Satterfield, <https://orcid.org/0000-0003-4787-7523>; Roberts-Hugghis,

<https://orcid.org/0000-0002-7844-263X>; Barley, <https://orcid.org/0000-0003-1675-6577>;
Borstein, <https://orcid.org/0000-0002-7258-141X>; Wainwright, <https://orcid.org/0000-0003-0498-4759>.

Short title: Functional Evolution of Cichlids

Keywords: geometric morphometrics, kinematics, morphology, adaptive radiation, cichlids

Article type: Major Article

ABSTRACT

Adaptive radiations highlight the mechanisms by which species and traits diversify and the extent to which these patterns are predictable. We used 1,110 high-speed videos of suction feeding to study functional and morphological diversification in 300 cichlid species from three African Great Lake radiations of varying ages (Victoria, Malawi and Tanganyika) and an older, spatially dispersed continental radiation in the Neotropics. Among African radiations, standing diversity was reflective of time. Morphological and functional variance in Lake Victoria, the youngest radiation, was a subset of that within Lake Malawi, which itself was nested within the older Tanganyikan radiation. However, functional diversity in Neotropical cichlids was often lower than in Lake Tanganyika, despite being much older. These two radiations broadly overlapped, but each diversified into novel trait spaces not found in the youngest lake radiations. Evolutionary rates across radiations were inversely related to age, suggesting extremely rapid trait evolution at early stages, particularly in lake radiations. Despite this support for early bursts, other patterns of trait diversity were inconsistent with expectations of adaptive radiations. This work suggests that cichlid functional evolution has played out in strikingly similar fashion in different radiations, with contingencies eventually resulting in lineage-specific novelties.

Introduction

Adaptive radiations provide glimpses into how traits diversify and evolve across related taxa in the presence of ecological opportunity (Simpson 1953; Gillespie et al. 2020). Studies on adaptive radiations have helped to explain how Caribbean anoles (Losos et al. 1998) and Hawaiian spiders (Gillespie 2004) have colonized new island habitats through repeated evolution of convergent ecomorphs. They have also highlighted mechanisms underlying trait divergence

across adaptive peaks in Bahamian pupfishes (Patton et al. 2022), Galapagos finches, and Hawaiian honeycreepers (Tokita et al. 2016). A common theme in the literature on adaptive radiations is the degree to which trait evolution reflects predictable patterns of diversification versus the generation of novel phenotypic combinations, where replicated radiations provide insights into these patterns (e.g., Schlüter 1996; Losos et al. 1998; Gillespie 2013).

Cichlid fishes are renowned for having multiple expansive radiations involving hundreds of species in each of three large African lakes – Victoria, Malawi and Tanganyika – (Freyer and Illes 1972; Stiassny & Meyer 1999; Seehausen 2006) and a continental radiation in tropical South and Central America (López-Fernández et al. 2013; Arbour and López-Fernández 2014). The existence of these large radiations of related species provides an opportunity to capitalize on natural replication to address questions about the evolutionary repeatability of these systems at a scale beyond the first few niche expansions. The radiations also differ considerably in age, approximately 55 Ma for Neotropical cichlids, 10 Ma for Lake Tanganyika, 2 Ma for Lake Malawi, and 0.1 Ma for Lake Victoria (we discuss cichlid ages further in the supplement). These differences present temporally spaced sample points that allow insight into the long-term unfolding of adaptive radiations and the relative importance of time and rate of diversification on current patterns of diversity.

Previous comparisons of phenotypic diversity in the three African lakes have drawn two main conclusions. First, diversity of body shape and trophic morphology differs between the radiations, with the oldest in Lake Tanganyika housing greater diversity of body shape and craniofacial morphology, and the youngest radiation in Lake Victoria, having the lowest diversity (Young et al. 2009; Cooper et al. 2010). It is not known whether adaptive radiations of the African lakes have amassed greater morphological diversity, and associated functional

variation, than the much older continental radiation in the Neotropics that includes roughly 500 species (Lopez-Fernandez et al. 2013). Second, convergent ecology and morphology are common both among and within radiations (Salzburger 2009), suggesting relatively predictable modes of diversification and broadly repeated patterns of evolution in feeding morphology (Hulsey et al. 2008; Cooper et al. 2010, Conith & Albertson 2019), body shape (Kocher et al. 1993; Young et al. 2009), or both (Rüber & Adams 2001; Muschick et al. 2012). Similar instances of convergence have been found among related groups of Neotropical cichlids (Burress et al. 2017; Arbour et al 2020), as well as between Neotropical and African species (Winemiller et al. 1995). Thus, large cichlid adaptive radiations could generate similar, though not identical, sets of phenotypes where diversity accumulates over extended time periods.

The temporal sampling of cichlid radiations creates an opportunity to evaluate, at various stages of progression, patterns of functional diversification relative to our expectations of adaptive radiations. A classic prediction is an early burst in trait diversification, where evolutionary rates are initially rapid as open niches in newly colonized habitats are filled, followed by a nonlinear decay in rates after initial expansion (Simpson 1953). An assumption of the early burst model is that the rapid increase in trait diversity is achieved by different lineages evolving toward separate adaptive zones where they subsequently undergo further diversification, resulting in comparatively greater variance among clades than within (Simpson 1953; Harmon et al. 2003).

In the present study, we describe the diversity of cichlid prey capture kinematics using high-speed video recordings of 300 species, sampled from the three African Great Lake radiations and the Neotropics. We contrast kinematic and morphological variation of the feeding mechanism in radiations of varying age to test the hypothesis that differences in standing

functional diversity are due to time, as opposed to different rates of evolution. To assess the repeatability and predictability of cichlid adaptive radiation, we also quantify the extent to which each has produced similar ranges of feeding kinematics. Additionally, we test the key expectation that adaptive radiations exhibit an early burst in trait diversification that is achieved through the partitioning of traits among clades (Simpson 1953; Harmon et al. 2003).

A secondary objective of this work is to examine the relationship between morphological and functional diversity of the cichlid feeding mechanism. Preliminary estimates of body and craniofacial variation in the three large African lake radiations have typically been interpreted as reflecting functional diversity linked to locomotor and feeding biomechanics (Young et al. 2009; Cooper et al. 2010). In many cases, links between morphological variation and functional properties are well-established (Hulsey & García de León 2005; Hulsey et al. 2006; Higham et al. 2007). Nevertheless, our current understanding of functional diversity in cichlids is largely inferred from morphological variation, rather than direct measurements of functional traits. Comparisons of functional diversity allow us to test the reliability of morphological variation to reflect function and help to identify key axes of diversification that are cryptic when only morphology is considered.

Methods

Species sampling and feeding videos

1,110 high-speed videos of feeding motions from 300 species of lab-filmed cichlids were studied (Tables S1 & S2). Species were broadly distributed phylogenetically from one of four focal radiations, three African Great Lakes, Victoria (n=40), Malawi (n=86), and Tanganyika (n=89), and the Neotropics (n=85 species). We note that two study species belonging to the Lake

Victoria Region Superflock, *Harpagochromis* sp. “golden duck” and *Pyxichromis orthostoma*, are endemic to Lake Kyoga, which retains a connection to Lake Victoria via the Victoria Nile River. All videos were filmed from a lateral perspective at 2,000 frames-per-second (McGee et al. 2016) and contained full-effort suction feeding strikes on moderately evasive, living midwater prey. Primary prey included mosquito larvae (*Culex pipiens*), black worms (*Lumbriculus* sp.), and *Daphnia magna*. Small fish were occasionally used as prey to elicit sufficiently full effort feeding strikes from some species, which was important for reducing kinematic variation due to fish effort. Videos in which fishes displayed low-effort prey capture behaviors were not included in this study. We extracted 10 frames from each video, equally spaced in time from the initiation of the motion to peak expansion of the feeding apparatus, prior to mouth closing. For comparative analyses, we matched filmed species to a recent cichlid phylogeny (McGee et al. 2020; Supplementary Information).

Morphological and functional traits

Cichlid functional diversity was determined using a variety of kinematic traits, all derived from a set of 10 landmarks and 8 semilandmarks manually placed on cranial images for each of 10 video frames comprising a motion (figs. 1 & S1). Digitizing was done in tpsDIG2 (Rohlf 2015) and StereoMorph (Olsen and Westneat 2015). Landmark data for 53 species came from a previous study (Martinez et al. 2018) but the remaining 247 species comprised new data. First, subsets of landmarks were used to measure movements (i.e., maximum excursions) of key morphological features involved in prey capture. In total, we created six *motion component* traits (fig. 1B), three from rotational movements of bones (*lower jaw rotation*, *cranial rotation*, *maxillary rotation*) and three from linear displacements (*premaxilla protrusion*, *hyoid*

depression, mouth gape). We analyzed these traits as a multivariate combination of all *motion components*, as well as individually. Due to the incommensurability of angles and linear displacements (Huttegger and Mitteroecker 2011), we converted the three rotational traits to distances by using the observed angle of rotation and the length of the rotating arm (measured on the fish at full gape) to determine the length of the arc transcribed by the structure in question (e.g., the Euclidean distance traveled by the distal end of the maxilla). All component traits were then scaled by dividing values by the centroid size of the fish's head in a closed-mouth state. Lastly, we averaged the components across repeated feeding trials within individuals, and then across individuals to get a mean trait value for the species. All additional traits described below were similarly averaged to species for comparative analyses.

Additional kinematic traits were created using an approach that characterizes movements as trajectories of shape change (fig. 1), integrating the numerous moving parts involved in a complex motion into a single object that allows for comparisons at the whole-motion level (Adams and Cerney 2007; Adams and Collyer 2009; Collyer and Adams 2013; Martinez et al. 2018; 2022; Martinez and Wainwright 2019). Digitized cranial landmarks were aligned and scaled using generalized Procrustes analysis (GPA) with the ‘gpagen’ function in the ‘geomorph’ package, v 4.0.3, in the R statistical environment, v 4.1.3 (Adams et al. 2021; R Core Team 2022), with alignment of sliding semilandmarks along the ventral margin of the head achieved by minimizing Procrustes distances. Once aligned with GPA, the progressive movements of landmark-tracked cranial features result in a trajectory of shape change (fig. 1A & E), the features of which can be used as traits that capture motion variation (Martinez and Wainwright 2019; Martinez et al. 2018; 2022). In this study, for example, the length of each motion trajectory is a measure of cranial *kinesis*, or the amount of movement generated by the feeding apparatus

during prey capture (fig. 1D). The total trajectory length was computed as the sum of Procrustes distances between consecutive motion shapes (Collyer and Adams 2013).

We also generated two composite traits designed to provide context about when and how kinesis is achieved. *Kinesis skew* was the ratio of kinesis across the final five motion shapes to the total kinesis for the motion, normalized by taking the natural logarithm for statistical analyses. This trait is a descriptor of the temporal distribution of kinesis within a movement, with smaller values indicating comparatively more movement toward the beginning of the feeding strike and larger values meaning that movement is concentrated near the end of the strike. Next, we measured a *kinesis coefficient* trait, as an analog to kinematic transmission (Westneat 1994; 2004), which is commonly used with biomechanical linkage models to describe output movement of an anatomical feature, given a degree of input motion from another. Here, we took the natural logarithm of total kinesis for a motion (output movement) divided by maximum cranial rotation (input movement) from the *motion components* described above. We used cranial rotation, which is powered by contraction of epaxial muscles posterior to the head, for the input value as it facilitates expansion of the buccal cavity and drives movements of other features of the feeding apparatus (Camp et al. 2020).

The final functional trait we compared was *motion pattern*, briefly described here. For complex biomechanical systems composed of numerous mobile features, any change in relative timing and/or degree of movement across those features causes variation in the pattern of movement at the whole-motion level. We used anatomical landmarks to express feeding movements as an ordered series of changing shapes over time, or a trajectory through morphospace (fig. 1A). The paths forged by these trajectories each have their own shape and represent *motion pattern* – different trajectory shapes represent different patterns of movement

that can be observed both within a single species feeding with different modes of prey capture (Martinez et al. 2022) and across species with divergently evolved feeding systems (Martinez et al. 2018). *Motion components* and *motion pattern* are both multivariate descriptors of feeding movements but capture contrasting aspects of their diversity. *Motion components* measure maximum excursions of key features of feeding motions, whereas *motion pattern* describes how and when those movements take place (Martinez et al. 2022). To compare *motion patterns*, we used modified code from the ‘trajectory.analysis’ function in the R package ‘RRPP’ (version 1.0.0) to align and scale trajectories (fig. S2; Collyer and Adams 2018; 2019). Here, the centroid size of the entire trajectory was the scaling factor.

To provide context to functional and kinematic patterns, we also examined interspecific cranial morphologies across cichlid species. We extracted head shape data from the starting positions of feeding motions, where the mouths were in a closed state. A separate shape alignment was done on head shape landmarks, which were then averaged to species prior to statistical analyses.

Trait diversity and overlap among radiations

Variance of morphological and kinematic traits, both univariate and multivariate, were measured and statistically compared using the ‘morphol.disparity’ function in ‘geomorph’ with 10,000 permutations. In addition to variance, a measure of trait dispersion, we were interested in the degree of overlap (or lack thereof) of trait ranges between radiations as a means of describing the occupation of multivariate functional and morphological spaces. We created four-dimensional hypervolumes for *motion components*, *motion pattern*, and head shape data using the R package ‘hypervolume’ v 3.0.0 (Blonder et al. 2014; 2018). We took the first four axes

from a principal component analysis, as hypervolumes are best conducted on orthogonal variables (Blonder et al. 2014; 2018). Hypervolumes were made for each radiation (e.g., species from Lake Tanganyika), and for subsets of the data excluding each radiation (e.g., all species *not* from Lake Tanganyika). We then assessed hypervolume overlap and the fraction of unique space occupied by each radiation. Lastly, we estimated the likelihood of our observed results against a null distribution of hypervolumes generated by randomly permuting group assignments among species 10,000 times (e.g., Corn et al. 2022).

Rates of evolution

For all traits, we estimated rates of evolution in each cichlid radiation with the ‘compare.evol.rates’ function in ‘geomorph’. This function computes the Brownian rate parameter for both univariate and multivariate continuous trait data using distance matrices (Adams 2014). The approach has been shown to yield numerically equivalent rate estimates to covariance-based methods for univariate data, but also accommodates high dimensional data, like shapes (Adams 2014). Pairwise comparisons of rates were accomplished through permutations in which trait data was randomly assigned to tips. Statistical significance was then assessed by comparing observed rate ratios between pairs of radiations to the distribution of ratios obtained from 10,000 permutations.

Rates were estimated using a tree containing all four radiations examined in this study (McGee et al. 2020) to maintain a single, consistent phylogenetic hypothesis. This tree reconstructs the age of the Lake Tanganyika radiation at about 28 million years old. To ensure that the resulting rates did not bias comparisons across radiations, or our interpretations of them, we additionally estimated rates for Lake Tanganyika using a time-calibrated tree based on

whole-genomes that dates the radiation to 10 Ma (Ronco et al. 2021). This tree was reconstructed with nearly all species of the *in situ* Tanganyikan radiation, so we trimmed it to our study species.

Modes of trait diversification

We examined both historical reconstructions of trait diversification and contemporary patterns of variation to explore the manner by which trait diversity was attained in cichlid radiations. We estimated the accumulation of trait disparity through time (DTT) in radiations using the ‘dtt’ function in the R package ‘geiger’ v 2.0.7. (Harmon et al. 2008; Pennell et al. 2014). DTT plots show relative disparities among subclades at each divergence event in the tree, estimating whether trait diversity is concentrated within or among subclades as an explicit test of the early burst expectation (Simpson 1953). An output of this analysis is the morphological disparity index (MDI), a metric for comparing the difference between the estimated relative disparity of a clade and the disparity of the clade under simulated Brownian motion. MDI statistics were calculated for the first 75% of the tree’s history, as missing species in the recent phylogeny may obscure patterns close to the present. We estimated DTT from subtrees of each radiation for *motion components*, *motion pattern* and head shape, using the first four axes from PCAs on each, consistent with our comparisons of hypervolumes. Tree topology is key to DTT analyses, so we note caution in interpreting results for young radiations, like Lakes Malawi and Victoria, in which a tree-like model of lineage diversification is unlikely due to widespread hybridization (Joyce et al. 2011; Meier et al. 2017; Scherz et al. 2022). Consequently, we focus our discussion on the two older radiations in Lake Tanganyika and the Neotropics but provide results for all radiations in the supplement materials.

To further examine patterns of trait dispersion, we computed distances between extant species and radiation-specific ancestral states. For each cichlid radiation, we estimated ancestral states under Brownian motion with the ‘gm.prcomp’ function in ‘geomorph’, extracting the value at the root of the tree as the most recent common ancestor (MRCA) for the radiation. Finally, we measured Euclidean distances (for *motion components*) and Procrustes distances (for *motion pattern* and head shape) between each species and its radiation’s MRCA.

Results

Functional diversity across cichlid radiations

Motion components, composed of six key features of fish cranial movement during feeding (fig. 1B), displayed 3.2 (Lake Tanganyika) and 2.9 times (Neotropics) greater variance in older radiations compared to the youngest radiation in Victoria (figs. 2 & 3; table S3). Separate univariate analyses on the individual components did show some variation in rank orders of variances across traits (fig. 2; table S3). In all cases, Lake Victoria had the lowest variance, followed closely by Lake Malawi, but some traits displayed their highest variation in Lake Tanganyika (*premaxillary protrusion*, *maxillary rotation*, *lower jaw rotation*, and *mouth gape*), while others were most variable in the Neotropics (*cranial rotation* and *hyoid depression*).

Functional traits derived from trajectories of shape change also showed different levels of diversity across radiations. Cranial *kinesis* had significantly greater variance in Lake Tanganyika than all other cichlid radiations, having 1.9-times greater variance than the next closest (the Neotropics) and 2.9-times greater variance than the lowest (Lake Victoria). *Kinesis skew*, the proportion of kinesis in the latter half of the feeding motion, was again most variable in Lake Tanganyika, but there was greater parity between it, Lake Malawi and the Neotropics (fig. 2).

Kinematic coefficient, output kinesis relative to input movement from cranial rotation, showed the highest variance in the Neotropical radiation, which was significantly greater than that of the younger radiations in Lakes Malawi and Victoria (fig. 2). Finally, the rank order of variances for whole *motion pattern*, a trait describing the timing and sequence of motion events, was the same as they were for *kinesis skew* – Lake Victoria was significantly lower than the other major radiations, followed by nearly identical values in Lake Malawi and the Neotropics, and the greatest variance again in Lake Tanganyika (fig. 2 & 3). Despite its young age, Lake Malawi showed surprisingly high diversity in *motion pattern*. This appears to be driven by a collection of species like *Tyrannochromis nigriventer*, *Copadichromis virginalis*, and *Caprichromis liemi* that have feeding motions in which kinesis is disproportionately concentrated toward the end of the strike (i.e., high *kinesis skew*, and *motion patterns* with large positive PC 1 scores in fig. 3B).

Occupation of novel functional spaces

Comparisons of hypervolumes identified whether individual radiations occupied unique regions of multivariate functional spaces. For the *motion components*, we found that 62% of Lake Tanganyika's and 49% of the Neotropics' functional space was unique to those radiations at the exclusion of all others, with both results occurring in the 99th percentile of randomized trials (fig. 3A; table S4). Cichlids occupying unique regions of the *kinematic components* functional space in Tanganyika included several specialized planktivores with high upper jaw protrusion in the genus *Cyprichromis* and elongate species with comparatively small gapes, like *Chalinochromis brichardi* and *Julidochromis dickfeldi*. In the Neotropics, multiple species of *Amatitlania* and a host of species in the tribe Geophagini (all with relatively small mouths, low cranial rotation, and low hyoid depression) occurred in one unique region, and species capable of

extreme upper jaw protrusion, *Petenia splendida* and *Caquetaia myersi*, were found in another. In contrast to Tanganyika and the Neotropics, only 6% of this space in Lake Malawi and 3% in Lake Victoria was unique to those lakes, suggesting that most of their diversity is nested within the other cichlid radiations (fig. 3A; table S4).

Across all species, the diversity of *motion patterns* was largely restricted to a distinct concave or arched distribution (fig. 3B). This likely reflects a general constraint on motion diversity – despite differences in the relative magnitude of movements (*motion components*), patterns of feeding movements in cichlids are created by the same morphological features, moving in the same direction, and mostly in the same sequence. One extreme of the *motion pattern* distribution was characterized by an abrupt shift in the direction of cranial shape change within morphospace toward the end of the motion, which manifested as an asymmetrical trajectory shape (left side of fig. 3B). During feeding sequences, this was caused by late onset cranial rotation and hyoid depression after full protrusion of the upper jaw was achieved, presumably for continued buccal expansion posteriorly to prolong suction during prey acquisition. The other extreme contained symmetrically shaped trajectories in which the rate of cranial shape change was slow initially but fast toward the end of the strike, such that kinesis was disproportionately concentrated in later motion stages (right side of fig. 3B), a pattern reminiscent of high *kinesis skew*. Comparisons of hypervolumes for *motion pattern* revealed a mostly nested pattern in which Tanganyika (54%) occupied the greatest volume of unique space (upper 99th percentile of permutations), with much lower values for the Neotropics (26%), Malawi (14%), and Victoria (1%; table S4).

Rates of functional evolution

Across all functional traits, there was a strong inverse and nonlinear relationship between rates and radiation ages (fig. S3; table S5). In each case, Lake Victoria had much higher rates than other radiations, ranging anywhere from 42 to 95-fold faster diversification compared to the radiation with the lowest rates, the Neotropical cichlids. Similarly, the second youngest radiation, Lake Malawi, consistently had the second highest rates of trait evolution. Pairwise comparisons of rates between Lakes Victoria and Malawi were statistically significant at the $\alpha=0.05$ level for functional traits except for *hyoid depression* and *kinesis skew* (table S5). One caveat is that these analyses assume a tree-like pattern of lineage diversification, and so we limit our interpretation primarily to emphasize the vastly different time scales over which functional trait diversity has accumulated in these radiations. Comparisons between the two older radiations revealed that rates in Lake Tanganyika (estimated from the McGee et al. (2020) tree) were always higher than in the Neotropics, ranging from 1.1-fold to 4-fold differences. However, unlike other pairwise comparisons among radiations, those between Tanganyika and the Neotropics failed to yield significant differences for over half of the functional traits considered. Significant differences in rate of evolution in these two radiations were found for *premaxillary protrusion*, *kinesis skew*, *kinesis*, *motion components*, and *motion pattern*.

Rates for Lake Tanganyika computed with the phylogeny from Ronco et al. (2021) were between 1.4 and 2.7 times higher than those based on the McGee et al. (2020) tree (table S5), consistent with the younger reconstructed age of the radiation in the former. However, the rank order across radiations remained the same, regardless of tree, maintaining a clear trend of decreasing rate with radiation age (fig. S3). Given that rate estimates using the Ronco et al. (2021) tree did not impact interpretations of relative patterns across radiations, we focus our discussion on results from the McGee et al. (2020) tree that contained all radiations.

Modes of functional diversification

Disparity through time (DTT) analyses provided information about temporal patterns of diversification for two multivariate functional traits, *motion components* and *motion pattern*. In Lake Tanganyika and the Neotropics, neither trait displayed DTT trends that were statistically different from Brownian motion – the morphological disparity index (MDI), describing the deviation of observed DTT trends from the null expectation, was not statistically significant for either dataset (fig. 4; see table S6 for results from all radiations). However, while DTT trends for *motion components* largely stayed within the 95% range of simulated trait histories, those for *motion pattern* were above the Brownian expectation in all radiations, in some cases for prolonged durations, suggesting that trait variance was at times disproportionately concentrated within subclades. Notably, none of the functional DTT trends fell below the lower 95% range for Brownian motion, which would indicate a possible early burst of trait diversification (fig. 4).

Trait dispersion of extant species around radiation-specific most recent common ancestors (MRCA)s additionally captured patterns of trait space occupation across radiations at different stages of progression. Euclidean distances of *motion components* between species and MRCAs were continuously distributed for all radiations except Lake Victoria (fig. 4B), generally showing a single large cluster of species in functional space, and not multiple clusters that might suggest divergence across discrete adaptive peaks. In Lake Victoria, a handful of species with comparably low upper jaw protrusion formed a small secondary peak that was more distantly situated from the radiation's MRCA (observations in the upper left of the Lake Victoria distribution in fig. 3A). These species consisted mostly of herbivorous cichlids from the genus *Neochromis* and omnivores in the genus *Pundamilia*, possibly representing a (weakly) isolated

adaptive peak related to trophic ecology and jaw function. For *motion pattern*, Procrustes distances from radiation-specific MRCA were right-skewed, particularly in Lake Victoria and the Neotropics, seemingly reflecting the highly constrained distribution of the trait more than distinct adaptive zones (figs. 3B & 4D).

Cranial morphology and its relation to motion diversity

Interspecific variance in head shape was highest in Neotropical cichlids, but only marginally greater than in Lake Tanganyika (table S3). Still, the Neotropics boasted 2.3-times more head shape diversity than Lake Malawi and 2.7-times more than Lake Victoria. Pairwise comparisons of variances were statistically significant except between the two youngest radiations, Malawi-Victoria, and the two oldest, Neotropics-Tanganyika (table S3). Interestingly, the high head shape variance in the Neotropics did not directly translate to functional diversity, as Lake Tanganyika still had greater (but statistically similar) diversity in *motion components*, and significantly higher variance in *kinesis*, *motion pattern*, *premaxillary protrusion*, and *maxillary rotation* (fig. 5C-E).

Comparisons of hypervolumes for head shape revealed that 59% of cranial diversity in the Neotropics and 57% in Lake Tanganyika was unique to those regions, both observations occurring in the upper 99th percentile of randomized permutations (table S4). One of the things that made the Neotropics stand out was expansion towards deep-headed taxa, like *Sympodus discus* and *Pterophyllum scalare*, and several species in the genus *Amatitlania* that were not as extreme but still outside of the space occupied by cichlids in other radiations (fig. 5A, lower scores on PC 1). Some species from the African lake radiations occurred in a non-overlapping region of morphospace with the Neotropics that contained many small-mouthed benthic biting

and picking specialists, like *Tropheus brichardi*, *Melanochromis wochepa*, and *Chalinochromis popelini* (fig. 5A, lower scores on PC 2). In addition, Lake Tanganyika possessed a fair degree of unique morphologies varying broadly in direction of mouth orientation (fig. 5B), from upturned (e.g., *Haplotaxodon microlepis*) to downward deflecting profiles (e.g., *Xenotilapia ochrogenys*). Morphological diversity within Lakes Malawi and Victoria was almost entirely contained within the other regions, with only 5% and 3% unique morphospace occupation, respectively.

Rates of head shape evolution were again lowest in the older radiations (Neotropics and Lake Tanganyika), faster in Lake Malawi and much faster in Lake Victoria (fig. S3; table S5). All pairwise comparisons of rates were statistically significant (table S5). Like functional analyses, disparity through time (DTT) trends for head shape were statistically indistinguishable from a Brownian process (fig. S4; table S6). However, in the Neotropics the DTT trend dipped just below the 95% range for Brownian simulations briefly from 44-40 Mya, and again for an extended time from about 39 to 28 Mya (fig. S4). During these periods, head shape disparity was concentrated among clades at a level beyond the null expectation, likely representing evolution of clades towards different adaptive peaks.

Discussion

In this study, we provide the first quantitative comparison of functional diversity across four major cichlid radiations, leveraging a large comparative kinematics dataset to contrast patterns of adaptive diversification across vastly different temporal scales (many thousands of years to over 50 My) and spatial ranges (individual lakes versus continental scale). We show that standing functional diversity in African cichlids is strongly related to radiation age and displays a striking nested pattern in which trait spaces occupied in Lakes Victoria and Malawi were almost

fully contained within that of Lake Tanganyika. Somewhat surprisingly, functional variance in the much older, continental Neotropical radiation was lower than it was in Lake Tanganyika for many traits, making the high diversity in the latter all the more impressive. This suggests that diversifying forces have operated more effectively in Lake Tanganyika, and likely across the African Great Lakes, as compared to the largely riverine cichlids of Central and South America. Our results are consistent with recent work suggesting that many cichlid lake radiations beyond those examined in this study have experienced elevated rates of morphological evolution (Burress and Muñoz 2023).

Cichlid feeding systems and adaptive radiation

Cichlids have long served as a model system for understanding adaptive radiation (Stiassny and Meyer 1999; Seehausen 2006; Turner 2007), yet we recovered mixed evidence that functional diversification of their feeding systems adheres to traditional expectations of this process (Simpson 1953). A negative relationship was found between radiation age and rates of kinematic and morphological evolution (fig. S3), suggesting that phenotypic diversification proceeds fastest in early-stage radiations in a manner consistent with an early burst. Young cichlid radiations in Lakes Victoria and Malawi support modest levels of trait diversity but they have acquired it at an incredibly fast pace due to high speciation rates (Seehausen 2006).

In addition to an early burst of diversification, an assumption of adaptive radiations remains that trait variance will be distributed disproportionately among clades versus within them (Simpson 1953; Harmon et al. 2003). Though cranial morphology showed some hints of elevated divergence among lineages in the Neotropics (fig. S4), none of the examined morphological or functional DTT trends were statistically different from Brownian motion (table

S6). Further, trait dispersion of extant species around their MRCA was mostly continuous (fig. 4) with minimal evidence of clustering (i.e., discrete ecomorphs), a pattern largely consistent across radiations. One exception was found for *motion components* in Lake Victoria, which displayed a small secondary cluster of species with low values of jaw protrusion (fig. 4B), possibly representing divergence toward an adaptive peak associated with a substrate biting mode of feeding. That notwithstanding, comparably low trait variance in the two youngest radiations (fig. 2) are not suggestive of rapid divergence *among* lineages occupying distinct adaptive zones, where a significant portion of total potential diversity is achieved at initial stages of adaptive expansion.

Our study suggests that the diversification of feeding systems in cichlid adaptive radiations likely occurs by way of early burst, achieved not by adaptive divergence among clades, but through extremely rapid within-clade dispersion in incipient radiations. Previous research has predicted such patterns in cichlids as a possible outcome of transgressive segregation during widespread introgression – a common theme of emerging African lake radiations – paired with ecological opportunity in newly colonized habitats (Seehausen 2004; Meier et al. 2017; Irisarri 2018; Salzburger 2018; Meier et al. 2019; Selz and Seehausen 2019). Although we do not explicitly address the ecological dimensions across which diversification occurs, a large number of studies have linked morphological and functional evolution of the cichlid feeding apparatus with dietary diversity (e.g., Albertson et al. 2005; Hulsey and García De León 2005; López-Fernández et al. 2012; Soria-Barreto et al. 2019; Arbour et al. 2020). Additionally, previous work on Lake Malawi and Tanganyika cichlids suggests that feeding diversity is distributed continuously along an axis of prey evasiveness (Martinez et al. 2018), matching observed patterns in this study of time-dependent trait dispersion around radiation specific MRCAs (fig. 4). If the landscape of ecological opportunity was discontinuously or

sparserly distributed, for instance, it could pose challenges for a radiation diversifying via transgressive segregation since open adaptive zones are no longer adjacent to currently occupied zones, thereby reducing the probability that hybrid offspring happen upon a more distantly situated adaptive peak.

Clear evidence for early bursts appears to be the exception and not the rule in comparative trait data (Harmon et al. 2010). We found that no single radiation showed signs of an early burst for functional traits relating to prey capture, but that a trend *among* radiations strongly supported such a pattern. Previous work on the Lake Tanganyika radiation also failed to recover an early burst for morphological traits of the jaw system (Ronco et al. 2021). A contributing factor in these findings could be the natural time-dependency of macroevolutionary rate estimates (Harmon et al. 2021). Phylogenetic reconstructions of Lake Tanganyika cichlids contain comparatively few, long branches near the root (e.g. McGee et al. 2020; Ronco et al. 2021), but previous work has shown that the radiation experienced a burst in lineage diversification early in its history that was facilitated by hybridization (Salzburger & Sturmbauer 2002; Seehausen 2006; Irisarri et al. 2018), a pattern seen in Lakes Victoria and Malawi. In this context, we may think of young radiations as providing our best window into the mode of lineage (and trait) diversification that once characterized the early history of older radiations. In similar fashion, older radiations may be helpful for informing predictions of what is to come for young radiations.

Are we watching the same film?

Stephen Jay Gould famously contemplated what the diversity of life on earth might look like if we had the ability to start over and replay the tape of life (Gould 1991). Would it be

unprecedented and unrecognizable, or would we see familiar patterns as selection inevitably leads to diversification along predictable paths? Many others have since pondered this question (e.g., Lobkovsky and Koonin 2012; Blount et al. 2018; Orgogozo 2015). In one sense, evolution is constantly repeating its own version of this experiment at much smaller spatial and temporal scales – independent radiations in related groups of organisms provide replication and insight into evolutionary contingencies under conditions of varying similarity. A primary focus of this study was to examine whether four large cichlid radiations, each resulting in hundreds of species and celebrated levels of ecological and morphological variation, have generated similar patterns of functional diversity. Has diversification of feeding functional morphology played out following the same script in each radiation, or have they diversified along separate functional axes? The answer appears to be that both are true.

Considering, for a moment, only the three African lake radiations examined in this study, there is an argument to be made that both functional and morphological diversification have progressed in a similar fashion in each of the lakes. The high-dimensional spaces filled by *motion components*, *motion pattern*, and cranial shape data each show the younger radiations, Malawi and Victoria, occupying subspaces of the older and more diverse Tanganyikan radiation, with novelty only commonplace in the latter. This result is consistent with impressions of widespread convergence on trophic morphotypes in Lakes Malawi and Tanganyika (e.g., Stiassny 1981; Kocher et al. 1993; Stiassny & Meyer 1999; Conith et al., 2019; Ronco et al. 2021). Interestingly, the nested pattern indicates that convergence emerges as a consequence of time-dependent and continuously distributed trait expansion from a more or less common starting point – young lake radiations following in the footsteps of their older counterparts. Still, it is unclear if we were to fast-forward the Lake Victoria tape millions of years to the current age

of Lake Tanganyika, whether we would find a carbon-copy of that lake or if selection would eventually lead the Victorian radiation into unfamiliar functional and morphological spaces.

When we expand beyond the large African lake radiations to contrast their phenotypic and functional diversity for the first time with the large Neotropical radiation, a different story emerges. The two older radiations are more diverse than the others and each has invaded novel, radiation-specific regions of functional and morphological space. Tanganyika boasts species with unique combinations of *motion components*, including highly specialized planktivores (*Cyprichromis*) and benthic foragers (e.g., *Pseudosimochromis curvifrons*, *Telamatochromis vittatus*). In the Neotropics, some geophagine cichlids feed with a strongly sequenced kinematic pattern, partitioned between distinct jaw protrusion and cranial rotation phases (asymmetrical *motion patterns* toward the left of fig. 3B). Additionally, an innovation in select piscivorous species from the tribe Heroini (e.g., *Petenia splendida* and *Caquetaia myersi*) results in extreme levels of premaxillary protrusion (Waltzek and Wainwright 2003; Hulsey and García de León 2005) that places them in a unique region of *motion component* space (fig. 3A). Both Lake Tanganyika and the Neotropics contain cichlids with functional profiles that do not occur anywhere else, showing that radiations can eventually diverge from each other in key areas of diversification. These observations amplify questions about the contrasting landscapes of ecological opportunity experienced by lake versus continental radiations.

Morphology provides an imperfect index of functional diversity

The idea that morphological variation can be used as a proxy for functional diversity is commonly advanced, but the widespread presence of complex form-function relationships tests this assumption (e.g., Wainwright et al. 2005; Young et al. 2007; 2010; Lautenschlager et al.

2020). Neotropical cichlids, when compared to the Lake Tanganyika radiation, illustrate that high variance in cranial morphologies does not always result in greater functional diversity. The primary axis of morphological variation in the Neotropics involved differences between elongate and slender (e.g., *Crenicichla*) versus deep heads with steep cranial profiles (e.g., *Sympoduson*, *Pterophyllum*, *Uaru*), which are adaptations typically found in species living in fast flowing riverine environments and slow-moving water like lakes or floodplains, respectively (López-Fernández et al. 2013). It is therefore likely that an important source of variance in head shapes of Neotropical cichlids is due to selection on habitat-specific body shape, perhaps involving adaptation of the locomotor system. Complex form-function relationships, particularly in biomechanical systems with many cooperating components, can make for challenging comparisons between morphologies and motions, and impact how these traits accumulate during adaptive diversification (Alfaro et al. 2005). These findings suggest caution is warranted in attributing observed morphological variation in fish feeding systems to functional diversity.

Conclusions

Cichlids have captivated the attention of biologists and aquarists alike with their remarkable diversity, boasting seemingly endless combinations of body shapes, sizes, coloration patterns, diets, and behaviors. Each radiation examined in this study has amassed an impressive variety of morphological and functional diversity. Adaptive radiation of cichlids has produced modest diversity of feeding kinematics in Lakes Victoria and Malawi, while Lake Tanganyika has surpassed even the much older Neotropical radiation, suggesting that the forces driving diversification in Tanganyika outstrip those in the Neotropics. However, these patterns of diversity have been established on very different time scales. Rates of functional evolution range

from 40-95 times faster in Lake Victoria than in the Neotropics, supporting the notion that the African Great Lake radiations have experienced comparatively rapid evolutionary change. These observations suggest that while similarities exist, adaptive radiation of cichlid feeding kinematics has not always followed a common profile. Rather, evolutionary contingencies linked to time and biogeography explain varied patterns of morphological and functional diversification across this iconic group of fishes.

Acknowledgements

We thank Ed Burress and Sarah Friedman for their support and assistance during this project. We also thank Michael Collyer for engaging discussions on morphometrics. CMM was funded by the UC Davis Chancellor's Postdoctoral Fellowship Program. KAC was supported by an American Dissertation Fellowship from the American Association of University Women and a fellowship from the Achievement Rewards for College Scientists Foundation. ASRH was supported by the National Science Foundation with a Graduate Research Fellowship, Grant No. 1650042.

Statement of Authorship

CMM and PCW conceptualized the project. CMM, KAC, and PCW developed the methods. MDM and SRB recorded most of the videos of cichlid feeding events, and CMM contributed videos for the remaining species. CMM, KAC, SW, DS, ASRH, AB, and PCW digitized landmark data on video frames. CMM prepared and curated data and KAC ran statistical analyses. CMM and PCW wrote the paper with edits from all authors.

Data and Code Availability

Data associated with this study is available at the Dryad digital repository (<https://doi.org/10.5061/dryad.h18931zsh>), and R scripts can be found at Zenodo (<https://doi.org/10.5281/zenodo.8354124>). The phylogenetic tree used for comparative methods was from a previously published paper (McGee et al. 2020), also available at Dryad (<https://doi.org/10.5061/dryad.fn2z34tr0>).

Literature Cited

- Adams, D. C. 2014. Quantifying and comparing phylogenetic evolutionary rates for shape and other high-dimensional phenotypic data. *Systematic Biology* 63:166–177.
- Adams, D. C., and M. M. Cerney. 2007. Quantifying biomechanical motion using Procrustes motion analysis. *Journal of Biomechanics*. 40:437–44.
- Adams, D. C., and M. L. Collyer. 2009. A general framework for the analysis of phenotypic trajectories in evolutionary studies. *Evolution* 63:1143–54.
- Adams, D., M. Collyer, A. Kaliontzopoulou, and E. Baken. 2021. “Geomorph: Software for geometric morphometric analyses. R package version 4.0.” <https://cran.r-project.org/package=geomorph>.
- Albertson, R. C., J. T. Streelman, T. D. Kocher, and P. C. Yelick. 2005. Integration and evolution of the cichlid mandible: the molecular basis of alternate feeding strategies. *PNAS* 102:16287–16292.
- Alfaro, M. E., D. I. Bolnick, and P. C. Wainwright. 2005. Evolutionary consequences of many-to-one mapping of jaw morphology to mechanics in labrid fishes. *American Naturalist* 165:E140–E154.

- Arbour, J. H., and H. López-Fernández. 2014. Adaptive landscape and functional diversity of Neotropical cichlids: implications for the ecology and evolution of Cichlinae (Cichlidae; Cichliformes). *Journal of Evolutionary Biology* 27:2431–2442.
- Arbour, J. H., C. G., Montaña, K. O., Winemiller, A. A., Pease, M., Soria-Barreto, J. L., Cochran-Biederman, and H. López-Fernández. 2020. Macroevolutionary analyses indicate that repeated adaptive shifts towards predatory diets affect functional diversity in Neotropical cichlids. *Biological Journal of the Linnean Society* 129:844-861.
- Blonder, B., C. Lamanna, C. Violle, and B. J. Enquist. 2014. The n-dimensional hypervolume. *Global Ecology and Biogeography* 23:595–609.
- Blonder, B., C. B. Morrow, B. Maitner, D. J. Harris, C. Lamanna, C. Violle, B. J. Enquist, and A. J. Kerkhoff. 2018. New approaches for delineating n-dimensional hypervolumes. *Methods in Ecology and Evolution* 9:305–319.
- Blount, Z. D., R. E. Lenski, and J. B. Losos. 2018. Contingency and determinism in evolution: Replaying life's tape. *Science* 362:aam5979.
- Burress, E. D., and M. M. Muñoz. 2023. Phenotypic rate and state are decoupled in response to river-to-lake transitions in cichlid fishes. *Evolution* qpad143.
- Burress, E. D., L. Piálek, J. R. Casciotta, A. Almirón, M. Tan, J. W. Armbruster, and O. Ríčan. 2017. Island- and lake-like parallel adaptive radiations replicated in rivers. *Proceedings of the Royal Society B* 285:20171762.
- Camp, A. L., A. M. Olsen, L. P. Hernandez, and E. L. Brainerd. 2020. Fishes can use axial muscles as anchors or motors for powerful suction feeding. *Journal of Experimental Biology* 223:jeb225649.

- Collyer, M. L., and D. C. Adams. 2013. Phenotypic trajectory analysis: comparison of shape change patterns in evolution and ecology. *Hystrix* 24:75–83.
- Collyer, M. L., and D. C. Adams. 2018. “RRPP: An R package for fitting linear models to high-dimensional data using residual randomization.” <https://besjournals.onlinelibrary.wiley.com/doi/10.1111/2041-210X.13029>.
- Collyer, M. L., and D. C. Adams. 2019. “RRPP: Linear Model Evaluation with Randomized Residuals in a Permutation Procedure. R package version 1.0.0.” <https://CRAN.R-project.org/package=RRPP>.
- Conith, M. R., A. J., Conith, and R. C. Albertson. 2019. Evolution of a soft tissue foraging adaptation in African cichlids: roles for novelty, convergence, and constraint. *Evolution* 73:2072-2084.
- Cooper, W. J., K. Parsons, A. McIntyre, B. Kern, A. McGee-Moore, and R. C. Albertson. 2010. Benthopelagic divergence of cichlid feeding architecture was prodigious and consistent during multiple adaptive radiations within African rift lakes. *PLoS ONE* 5:e9551.
- Corn, K. A., S. T. Friedman, E. D. Burress, C. M. Martinez, O. Larouche, S. A. Price, and P. C. Wainwright. 2022. The Rise of Biting During the Cenozoic Fueled Reef Fish Body Shape Diversification. *Proceedings of the National Academy of Sciences* 119:e2119828119.
- Delvaux, D. 1995. Age of Lake Malawi (Nyasa) and water level fluctuations. Musée Royal Afrique Centrale, Tervuren (Belgique), Department de Géologie et Mineralogies, Rapport Annuel 1995-1996:99-108.
- Fryer, G., and T. D. Iles. 1972. The cichlid fishes of the Great Lakes of Africa. Oliver and Boyd, Edinburgh.

Gillespie, R. G. 2013. Adaptive radiation: convergence and non-equilibrium. *Current Biology*

2:R71-R74

Gillespie, R. 2004. Community assembly through adaptive radiation in Hawaiian spiders.

Science 303:356-359

Gillespie, R. G., G. M. Bennett, L. De Meester, J. L. Feder, R. C. Fleischer, L. J. Harmon, A. P.

Hendry, M. L. Knope, J. Mallet, C. Martin, and C. E. Parent. 2020. Comparing adaptive radiations across space, time, and taxa. *Journal of Heredity*, 111:1-20.

Gould, S. J. 1991. Wonderful life – the Burgess shale and the nature of history. WW. Norton & Company, New York.

Greenwood, P. H. 1980. Towards a phyletic classification of the 'genus' *Haplochromis* (Pisces, Cichlidae) and related taxa. Part 2; the species from Lakes Victoria, Nabugabo, Edward, George and Kivu. *Bulletin of the British Museum (Natural History) Zoology*. 39:1-101.

Harmon, L. J., J. B. Losos, T. J. Davies, R. G. Gillespie, J. L. Gittleman, W. B. Jennings, K. H. Kozak, M. A. McPeek, F. Moreno-Roark, T. J. Near, A. Purvis, R. E. Ricklefs, D. Schluter, J. A. Schulte II, O. Seehausen, B. L. Sidlauskas, O. Torres-Carvajal, J. T. Weir, and O. Mooers, A. 2010. Early bursts of body size and shape evolution are rare in comparative data. *Evolution*. 64:2385-2396.

Harmon, L. J., M. W. Pennell, L. F. Henao-Diaz, J. Rolland, B. N. Sipley, and J. C. Uyeda. 2021. Causes and consequences of apparent timescaling across all estimated evolutionary rates. *Annual Review of Ecology, Evolution, and Systematics* 52:587-609.

Harmon, L. J., J. A. Schulte, A. Larson, and J. B. Losos. 2003. Tempo and mode of evolutionary radiation in iguanian lizards. *Science* 301:961-964.

- Harmon, L. J., J. T. Weir, C. D. Brock, R. E. Glor, and W. Challenger. 2008. GEIGER: Investigating evolutionary radiations. *Bioinformatics* 24:129–131.
- Higham, T. E., C. D. Hulsey, O. Ríčan, and A. M. Carroll. 2007. Feeding with speed: prey capture evolution in cichlids. *Journal of Evolutionary Biology* 20:70-78
- Hulsey, C. D., and F. J. García De León. 2005. Cichlid jaw mechanics: linking morphology to feeding specialization. *Functional Ecology* 19:487-494.
- Hulsey, C. D., F. J. García De León, and R. Rodiles-Hernandez. 2006. Micro- and macroevolutionary decoupling of cichlid jaws: A test of Liem's key innovation hypothesis. *Evolution* 60:2096-2109.
- Hulsey, C. D., R. J. Roberts, A. S. Lin, R. Guldberg, and J. T. Streelman. 2008. Convergence in a mechanically complex phenotype: detecting structural adaptations for crushing in cichlid fish. *Evolution* 62:1587-1599.
- Huttegger, S. M., and P. Mitteroecker. 2011. Invariance and meaningfulness in phenotype spaces. *Evolutionary Biology* 38:335-351.
- Irisarri, I., P. Singh, S. Koblmüller, J. Torres-Dowdall, F. Henning, P. Franchini, C. Fischer, A. R. Lemmon, E. M. Lemmon, G. G. Thallinger, C. Sturmbauer, and A. Meyer. 2018. Phylogenomics uncovers early hybridization and adaptive loci shaping the radiation of Lake Tanganyika cichlid fishes. *Nature Communications* 9:3159.
- Joyce, D. A., D. H. Lunt, M. J. Genner, G. F. Turner, R. Bills, and O. Seehausen. 2011. Repeated colonization and hybridization in Lake Malawi cichlids. *Current Biology* 21:R108–R109.

Kocher, T. D., J. A. Conroy, K. R. McKaye, and J. R. Stauffer. 1993. Similar morphologies of cichlid fish in Lakes Tanganyika and Malawi are due to convergence. *Molecular Phylogenetics and Evolution* 2:158–165.

Lautenschlager, S., B. Figueirido, D. D. Cashmore, E.-M. Bendel, and T. L. Stubbs. 2020. Morphological convergence obscures functional diversity in sabre-toothed carnivores. *Proceedings of the Royal Society B* 287:20201818.

Lobkovsky, A. E., and E. V. Koonin. 2012. Replaying the tape of life: quantification of the predictability of evolution. *Frontiers in Genetics* 3:246.

López-Fernández, H., J. H. Abrbour, K. O. Winemiller, and R. L. Honeycutt. 2013. Testing for ancient adaptive radiation in Neotropical cichlid fishes. *Evolution* 67:1321-1337.

López-Fernández, H., K. O. Winemiller, C. Montaña, and R. L. Honeycutt. 2012. Diet-morphology correlations in the radiation of South American Geophagine Cichlids (Perciformes: Cichlidae: Cichlinae). *PLoS One*. 7:e33997.

Losos, J. B., T. R. Jackman, A. Larson, K. D. Queiroz, and L. Rodríguez-Schettino. 1998. Contingency and determinism in replicated adaptive radiations of island lizards. *Science* 279:2115-2118.

Martinez, C. M., Corn, K. A., Williamson, S., Satterfield, D., Roberts-Hugghis, A. S., Barley, A., Borstein, S. R., McGee, M. D., and Wainwright, P. C. Data from: Replicated Functional Evolution in Cichlid Adaptive Radiations. *American Naturalist*, Dryad Digital Repository, <https://doi.org/10.5061/dryad.h18931zsh>.

Martinez, C. M., Corn, K. A., Williamson, S., Satterfield, D., Roberts-Hugghis, A. S., Barley, A., Borstein, S. R., McGee, M. D., and Wainwright, P. C. Data from: Replicated Functional

Evolution in Cichlid Adaptive Radiations. American Naturalist, Zenodo Digital Repository, <https://doi.org/10.5281/zenodo.8354124>.

Martinez, C. M., M. D. McGee, S. R. Borstein, and P. C. Wainwright. 2018. Feeding ecology underlies the evolution of cichlid jaw mobility. *Evolution* 72:1645-1655.

Martinez, C. M., A. Tovar, and P. C. Wainwright. 2022. A novel intramandibular joint facilitates feeding versatility in the sixbar distichodus. *Journal of Experimental Biology* 225:jeb243621.

Martinez, C. M., and P. C. Wainwright. 2019. Extending the geometric approach for studying biomechanical motions. *Integrative and Comparative Biology* 59:684-695.

Matschiner, M. 2018 Gondwanan vicariance or trans-Atlantic dispersal of cichlid fishes: a review of the molecular evidence. *Hydrobiologia* 832:9-37.

Matschiner, M., A. Böhne, F. Ronco, and W. Salzburger. 2020 The genomic timeline of cichlid fish diversification across continents. *Nature Communications* 11:5895.

McGee, M. D., S. R. Borstein, J. I. Meier, D. A. Marques, S. Mwaiko, A. Taabu, M. A. Kishe, B. O'Meara, R. Bruggmann, L. Excoffier, and O. Seehausen. 2020. The ecological and genomic basis of explosive adaptive radiation. *Nature* 586:75-79.

McGee, M. D., B. C. Faircloth, S. R. Borstein, J. Zheng, C. D. Hulsey, P. C. Wainwright, and M. E. Alfaro. 2016. Replicated divergence in cichlid radiations mirrors a major vertebrate innovation. *Proceedings of the Royal Society B* 283:20151413.

Meier, J. I., D. A. Marques, S. Mwaiko, C. E. Wagner, L. Excoffier, and O. Seehausen. 2017. Ancient hybridization fuels rapid cichlid fish adaptive radiations. *Nature Communications* 8:14363.

Meier, J. I., R. B. Stelkens, D. A. Joyce, S. Mwaiko, N. Phiri, U. K. Schliewen, O. M. Selz, C. E.

Wagner, C. Katongo, and O. Seehausen. 2019. The coincidence of ecological opportunity with hybridization explains rapid adaptative radiation in Lake Mweru cichlid fishes. *Nature Communications* 10:5391.

Muschick, M. A. Indermaur, and W. Salzburger. 2012. Convergent Evolution within an Adaptive

Radiation of Cichlid Fishes. *Current Biology* 22:2362-2368.

Olsen, A., and M. Westneat. 2015. "StereoMorph: an R package for the collection of 3D landmarks and curves using a stereo camera set-up." *Methods in Ecology and Evolution* 6:351-356.

Orgogozo, V. 2015. Replaying the tape of life in the twenty-first century. *Interface Focus* 5:20150057.

Patton, A. H., E. J. Richards, K. J. Gould, L. K. Buie, and C. H. Martin. 2022. Hybridization alters the shape of the genotypic fitness landscape, increasing access to novel fitness peaks during adaptive radiation. *Elife* 11:e72905.

Pennell, M., J. Eastman, G. Slater, J. Brown, J. Uyeda, R. Fitzjohn, M. Alfaro, and L. Harmon. 2014. "geiger v2.0: an expanded suite of methods for fitting macroevolutionary models to phylogenetic trees." *Bioinformatics* 30:2216-2218.

R Core Team. 2022. R: A language and environment for statistical computing. R Foundation for Statistical Computing, Vienna, Austria. URL <https://www.R-project.org/>.

Rohlf, F. J. 2015. The tps series of software. *Histrix* 26:9–12.

- Ronco, F., M. Matschiner, A. Böhne, A. Boila, H. H. Büscher, A. El Taher, A. Indermaur, M. Malinsky, V. Ricci, A. Kahman, S. Jentoft, and W. Salzburger. 2021. Drivers and dynamics of massive adaptive radiation in cichlid fishes. *Nature* 589:76-81.
- Rüber, L., and D. C. Adams. 2001. Evolutionary convergence of body shape and trophic morphology in cichlids from Lake Tanganyika. *Journal of Evolutionary Biology* 14:325-332.
- Salzburger, W. 2009. The interaction of sexually and naturally selected traits in the adaptive radiations of cichlid fishes. *Molecular Ecology* 18:169-185.
- Salzburger, W. 2018. Understanding explosive diversification through cichlid fish genomics. *Nature Reviews Genetics* 19:705-717.
- Salzburger, W., and C. Sturmbauer. 2002. Speciation via introgressive hybridization in East African cichlids? *Molecular Ecology* 11:619-625.
- Scherz, M. D., P. K. Masonick, A. Meyer, and C. D. Hulsey. 2022. Between a rock and a hard polytomy: phylogenomics of the rock-dwelling mbuna cichlids of Lake Malawi. *Systematic Biology* 71:741-757.
- Schlüter, D. 1996. Adaptive radiation along genetic lines of least resistance. *Evolution* 50:1766-1774.
- Seehausen, O. 1996. Lake Victoria rock cichlids, taxonomy, ecology and distribution. *Verdijin Cichlids*, Zevenhuizen, Netherlands.
- Seehausen, O. 2004. Hybridization and adaptive radiation. *Trends in Ecology and Evolution* 19:198-207.
- Seehausen, O. 2006. African cichlid fishes, a model system in adaptive radiation research. *Proceedings of the Royal Society B* 273:1987-1998.

- Seehausen, O., E. Lippitsch, N. Bouton, H. Zwennes. 1998. Mbipi, the rock-dwelling cichlids of Lake Victoria: description of three new genera and fifteen new species (Teleostei). *Ichthyological Exploration of Freshwaters* 9:129-228.
- Selz, O. M., and O. Seehausen. 2019. Interspecific hybridization can generate functional novelty in cichlid fish. *Proceedings of the Royal Society B* 286:20191621.
- Simpson, G. G. 1953. The major features of Evolution. Columbia University Press, New York.
- Soria-Barreto, M., R. Rodiles-Hernández, and K.O. Winemiller. 2019. Trophic ecomorphology of cichlid fishes of Selva Lacandona, Usumacinta, Mexico. *Environmental Biology of Fishes* 102:985-996.
- Sparks, J. S. 2004. Molecular phylogeny and biogeography of the Malagasy and South Asian cichlids (Teleostei: Perciformes: Cichlidae). *Molecular Phylogenetics and Evolution*. 30:599–614.
- Sparks, J. S., and W. L. Smith. 2004. Phylogeny and biogeography of cichlid fishes (Teleostei: Perciformes: Cichlidae). *Cladistics* 20:501–517.
- Stager, J. C., and T. C. Johnson. 2008. The late Pleistocene desiccation of Lake Victoria and the origin of its endemic biota. *Hydrobiologia* 596:5-16.
- Stiassny, M. L. J. 1981. Phylogenetic versus convergent relationship between piscivorous cichlid fishes from Lakes Malawi and Tanganyika. *Bulletin of the British Museum (Natural History) Zoology*. 40:67-101.
- Stiassny, M. L. J., and A. Meyer. 1999. Cichlids of the rift lakes, *Scientific American* 280:64-69.
- Tokita, M., W. Yano, H. F. James, and A. Abzhanov. 2016. Cranial shape evolution inadaptive radiations of birds: comparative morphometrics of Darwin's finches and Hawaiian honeycreepers. *Philosophical Transactions of the Royal Society B* 372:20150481.

- Turner, G. F. 2007. Adaptive radiation of cichlid fish. *Current Biology* 17:R827-R831.
- Verheyen, E., W. Salzburger, J. Snoeks, A. Meyer. 2003. Origin of the superflock of cichlid fishes from Lake Victoria, East Africa. *Science* 300:325-329.
- Wainwright, P. C., M. E. Alfaro, D. I. Bolnick, and C. D. Hulsey. 2005. Many-to-one mapping of form to function: a general principle in organismal design? *Integrative and Comparative Biology* 45:256–262.
- Waltzek, T. B., and P. C. Wainwright. 2003. Functional morphology of extreme jaw protrusion in Neotropical cichlids. *Journal of Morphology* 257:96-106.
- Westneat, M. W. 1994. Transmission of force and velocity in the feeding mechanisms of labrid fishes (Teleostei, Perciformes). *Zoomorphology* 114:103-118.
- Westneat, M. W. 2004. Evolution of Levers and Linkages in the Feeding Mechanisms of Fishes. *Integrative and Comparative Biology* 44:378-389.
- Winemiller, K. O., L. C. Kelso-Winemiller, and A. L. Brenkert. 1995. Ecomorphological diversification and convergence in fluvial cichlid fishes. *Environmental Biology of Fishes* 44:235-261.
- Young, K. A., J. Snoeks, and O. Seehausen. 2009. Morphological Diversity and the Roles of Contingency, Chance and Determinism in African Cichlid Radiations. *PLoS ONE* 4:e4740.
- Young, R. L., T. S. Haselkorn, and A. V. Badyaev. 2007. Functional equivalence of morphologies enables morphological and ecological diversity. *Evolution* 61:2480–2492.
- Young, R. L., M. J. Sweeney, and A. V. Badyaev. 2010. Morphological diversity and ecological similarity: versatility of muscular and skeletal morphologies enables ecological convergence in shrews. *Functional Ecology* 24:556-565.

References Cited Only in the Online Enhancements

- Greenwood, P. H. 1980. Towards a phyletic classification of the 'genus' *Haplochromis* (Pisces, Cichlidae) and related taxa. Part 2; the species from Lakes Victoria, Nabugabo, Edward, George and Kivu. Bulletin of the British Museum (Natural History) Zoology. 39:1-101.
- Johnson, T. C., C. A. Scholz, M. R. Talbot, K. Kelts, R. D. Ricketts, G. Ngobi, K. Beuning, I. Ssemmanda, and J. W. McGill. 1996. Late Pleistocene desiccation of Lake Victoria and rapid evolution of cichlid fishes. Science 273:1091-1093.
- Ronco, F., M. Matschiner, A. Böhne, A. Boila, H. H. Büscher, A. El Taher, A. Indermaur, M. Malinsky, V. Ricci, A. Kahman, S. Jentoft, and W. Salzburger. 2021. Drivers and dynamics of massive adaptive radiation in cichlid fishes. Nature 589:76-81.

Figure Legends

Figure 1. Functional traits examined across 300 species of cichlid in this study. **A)** Principal component axes, PC 1 and PC 2, displaying shape change for a single trajectory composed of 10 cranial shapes during a suction feeding motion. **B)** Subsets of two or three landmarks were used to measure maximum excursions of six commonly measured *motion components* of suction feeding in percomorph fishes. **C)** Changes in the timing or extent of movements represent differences in *motion pattern* that are manifested as variation in trajectory shapes. Trajectories varied in spacing of cranial shape changes and the relative symmetry of trajectory paths. **D)** A series of trajectory-derived traits related to mobility, included cranial *kinesis* (total trajectory

length), *kinesis coefficient* (not pictured, total output kinesis divided by input movement from cranial rotation), and *kinesis skew* (kinesis over the last five motion shapes divided by total kinesis). **E)** PCs 1 and 2 from 1,110 trajectories of suction feeding motions, with deformation grids displaying shape change. All plots are shown in two dimensions for visualization, but data analysis was in the full dimensionality of the shape data unless otherwise noted.

Figure 2. Functional trait variances in cichlid adaptive radiations plotted against maximum radiation age. Six individual kinematic traits are shown on top, with an arrow pointing to the multivariate *motion components* containing all of them. *Motion pattern* (i.e., the shape of a kinematic trajectory) is shown in the middle with an arrow pointing to composite *kinesis-based* traits measured from trajectories. Letters next to plot points denote significant P-values from pairwise comparisons. Radiations sharing a letter do not have statistically different variances.

Figure 3. Primary dimensions of variation, PCs 1 and 2, from separate principal component analyses for species-averaged multivariate functional traits. **A)** *Motion components*, a dataset comprising measurements of maximum excursions for six key kinematic features are plotted by cichlid radiation. Representative drawings of cichlid heads at maximum gape are shown across the plot, and trait loadings are shown on the right. **B)** Variation in *motion patterns* by radiation, with two-dimensional representations of the shapes of kinematic trajectories provided at select locations of the plot (red diamonds). Low values on PC 1 are motions with an abrupt shift in the manner of cranial movements and large values are motions in which kinesis is disproportionately concentrated toward the end of the strike. For both multivariate traits, Lake Tanganyika and the Neotropics display unique occupation of this space, while Lakes Malawi and Victoria are almost

entirely nested within them. Estimated values of radiation-specific most recent common ancestors (MRCA) are shown as large dots with white borders.

Figure 4. Disparity through time (DTT) plots in the two oldest cichlid radiations, Lake Tanganyika and the Neotropics, for **A**) *motion components* and **C**) *motion pattern*. Also shown are distributions of **B**) Euclidean distances of *motion components* and **D**) Procrustes distances of *motion pattern* between extant species and their radiation-specific most recent common ancestor (MRCA).

Figure 5. Species-averaged interspecific head shape diversity across cichlid radiations. **A)** Major axes of variation, PCs 1 & 2, show the wide diversity of head shapes in Neotropical cichlids, most notably in head depth (left side of plot). Small-mouthed taxa in African lakes, often benthic biting feeders, are concentrated toward the bottom of the plot. **B)** PCs 3 and 4 display axes on which Lake Tanganyika contains high morphological diversity, including variation in orientation of jaws. Most recent common ancestors (MRCAs) for radiations are shown as large dots with white borders. **C-E)** Variance in head shape is shown in relation to select kinematic traits, displaying relationships between form and function. High morphological diversity in the Neotropics does not translate to commensurate kinematic diversity.

Figure 1

This is the author's accepted manuscript without copyediting, formatting, or final corrections. It will be published in its final form in an upcoming issue of The American Naturalist, published by The University of Chicago Press. Include the DOI when citing or quoting:
<https://doi.org/10.1086/731477>. Copyright 2024 The University of Chicago.

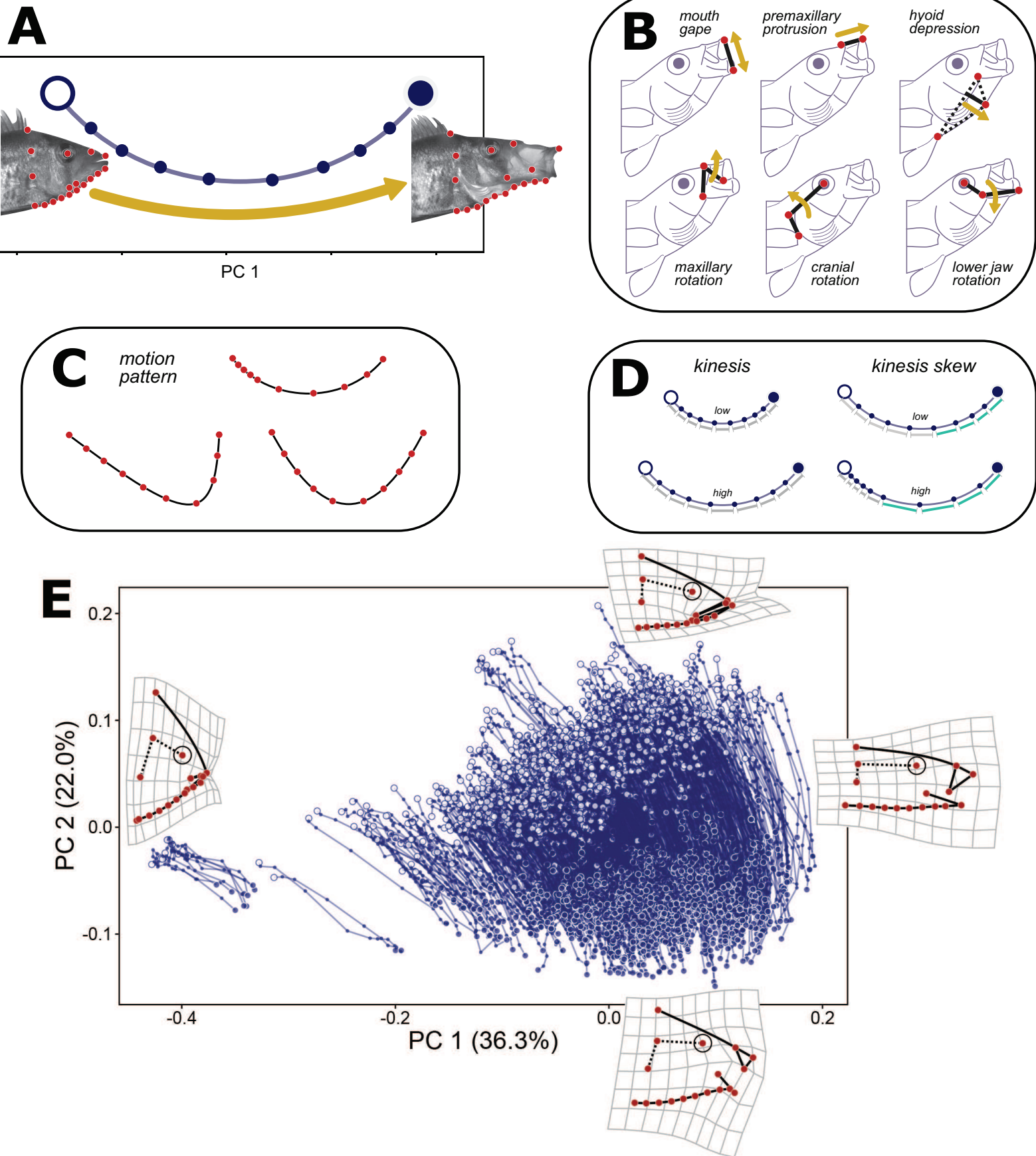


Figure 2

This is the author's accepted manuscript without copyediting, formatting, or final corrections. It will be published in its final form in an upcoming issue of The American Naturalist, published by The University of Chicago Press. Include the DOI when citing or quoting:
<https://doi.org/10.1086/731477>. Copyright 2024 The University of Chicago.

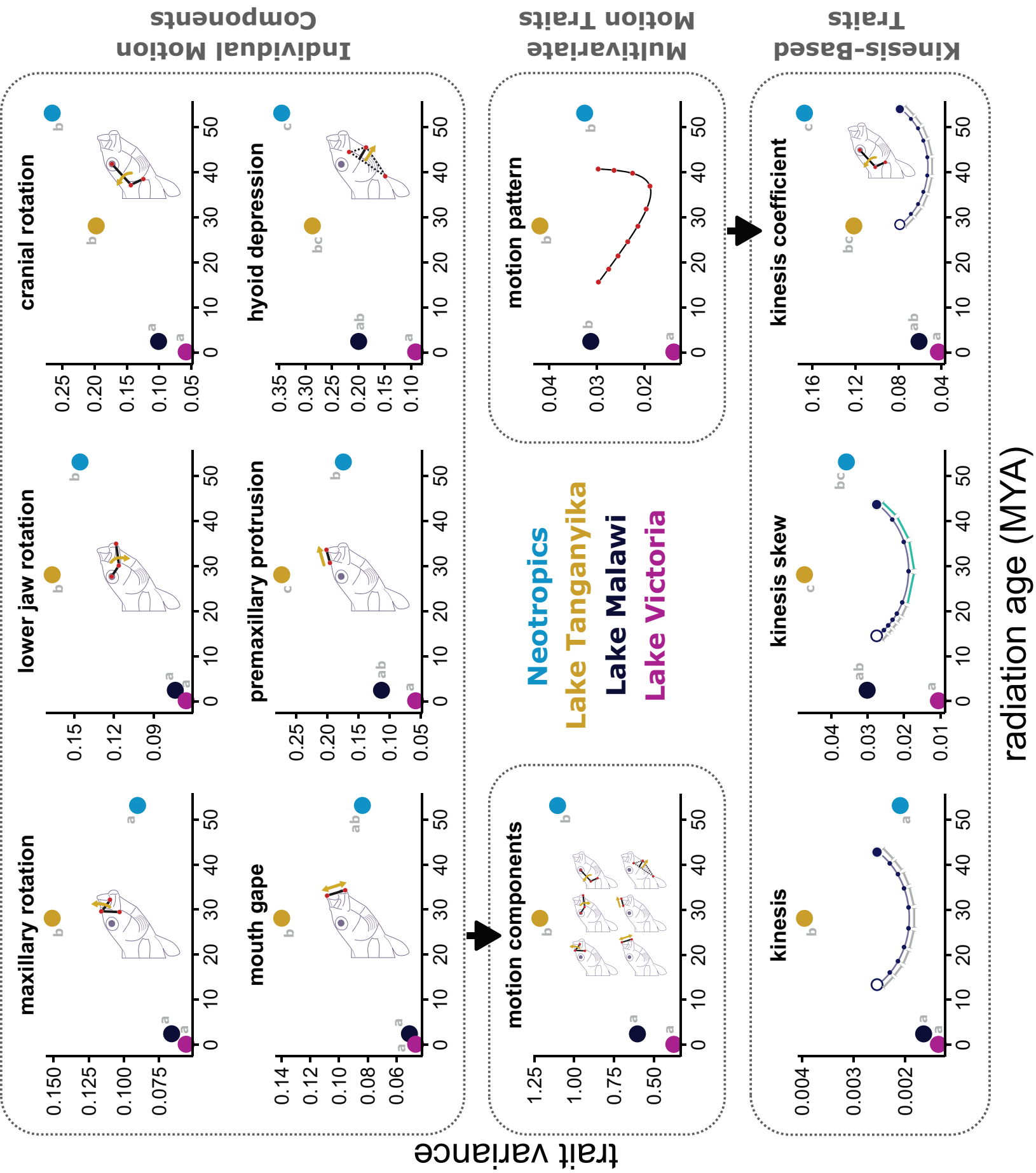


Figure 3

This is the author's accepted manuscript without copyediting, formatting, or final corrections. It will be published in its final form in an upcoming issue of The American Naturalist, published by The University of Chicago Press. Include the DOI when citing or quoting:
<https://doi.org/10.1086/731477>. Copyright 2024 The University of Chicago.

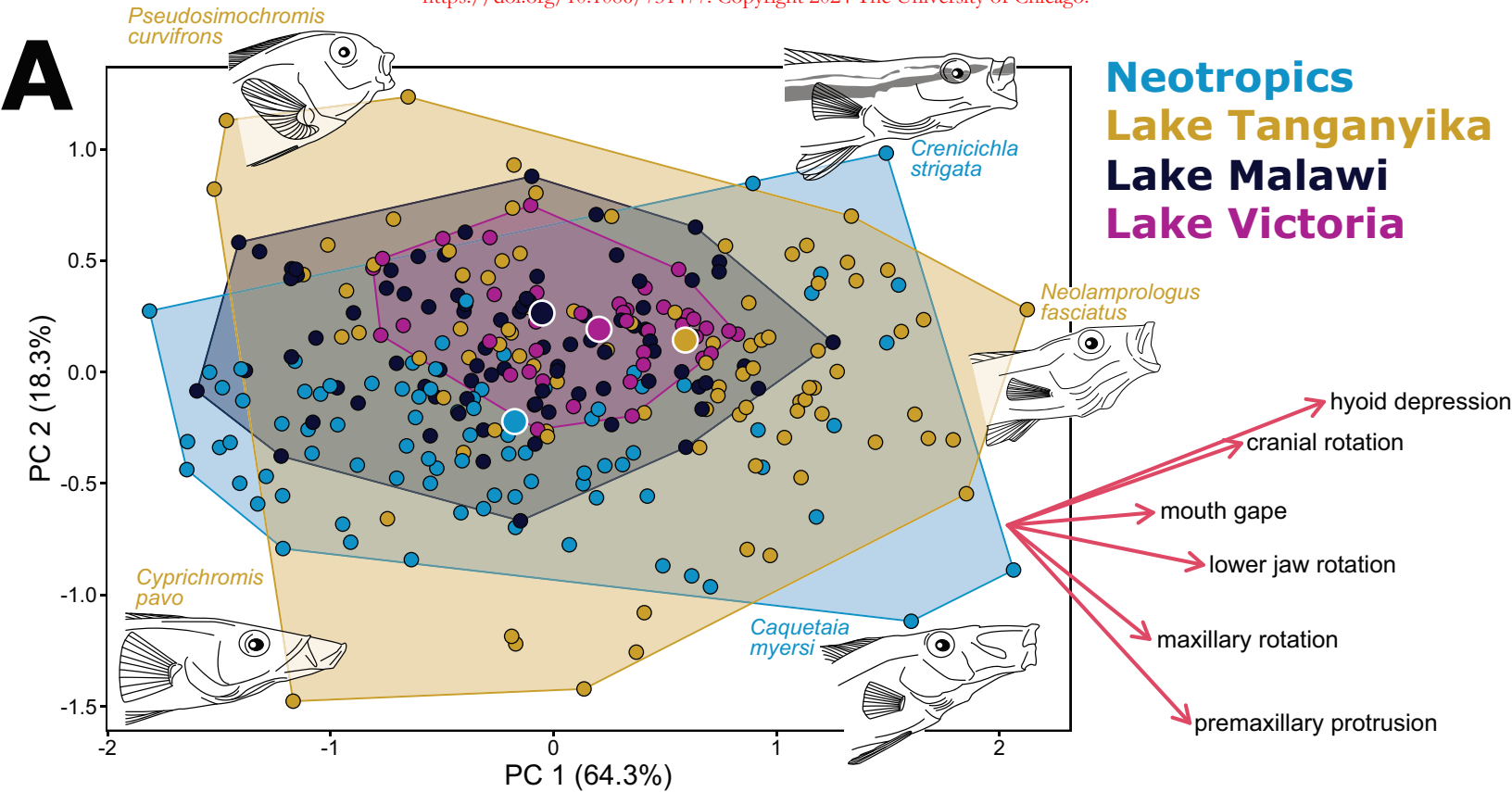
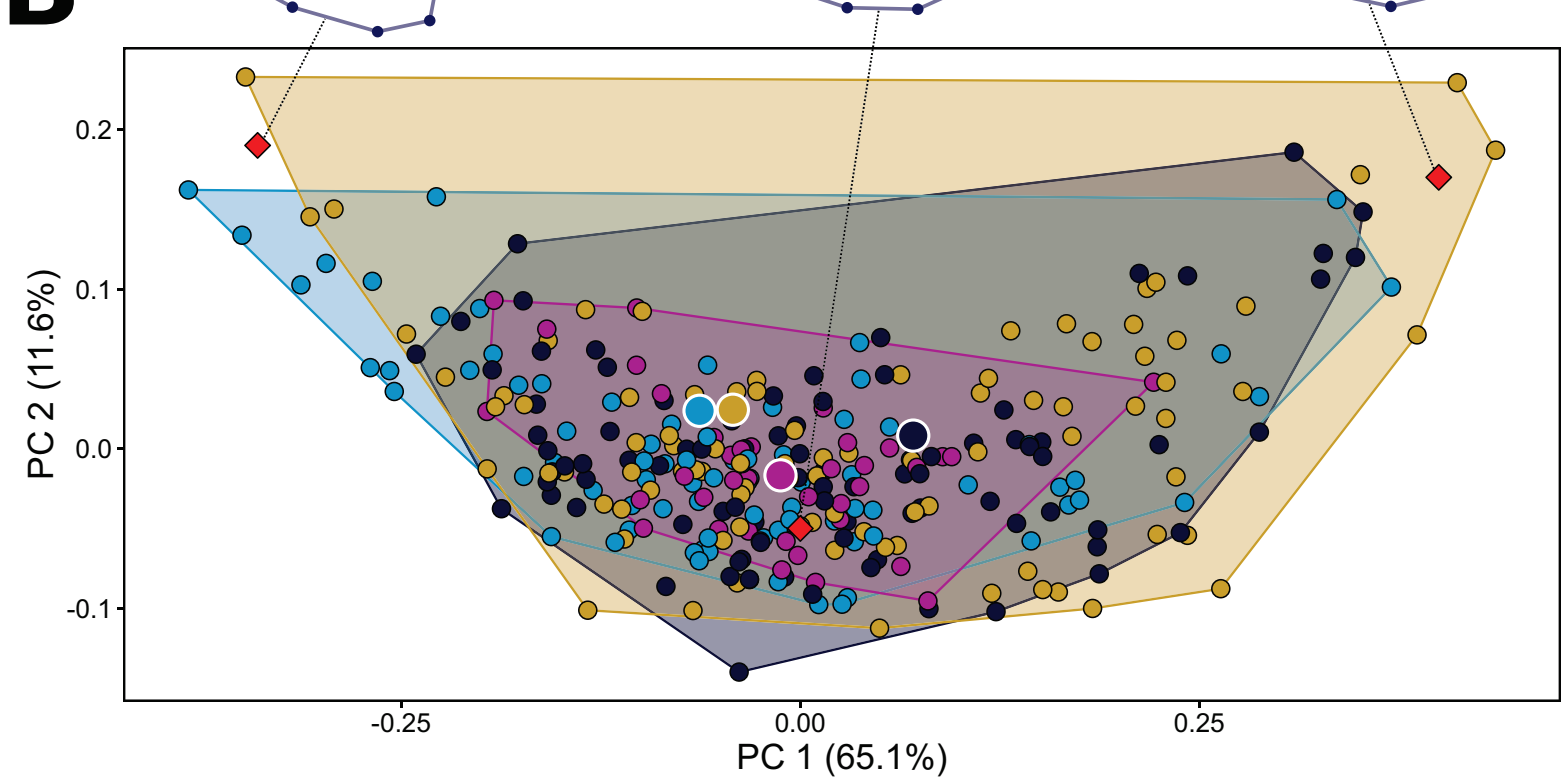
A**B**

Figure 4

This is the author's accepted manuscript without copyediting, formatting, or final corrections. It will be published in its final form in an upcoming issue of The American Naturalist, published by The University of Chicago Press. Include the DOI when citing or quoting:
<https://doi.org/10.1086/731477>. Copyright 2024 The University of Chicago.

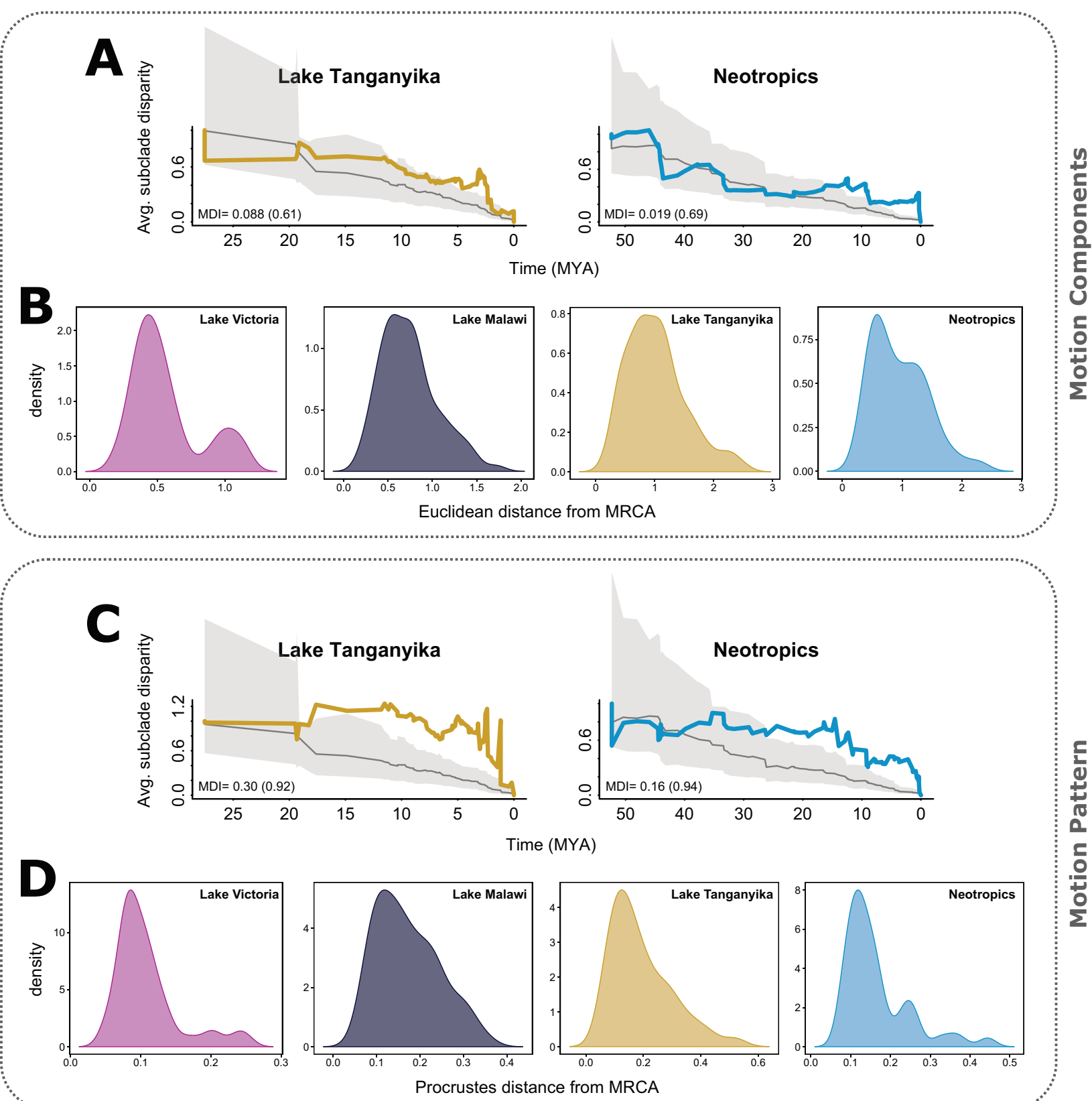
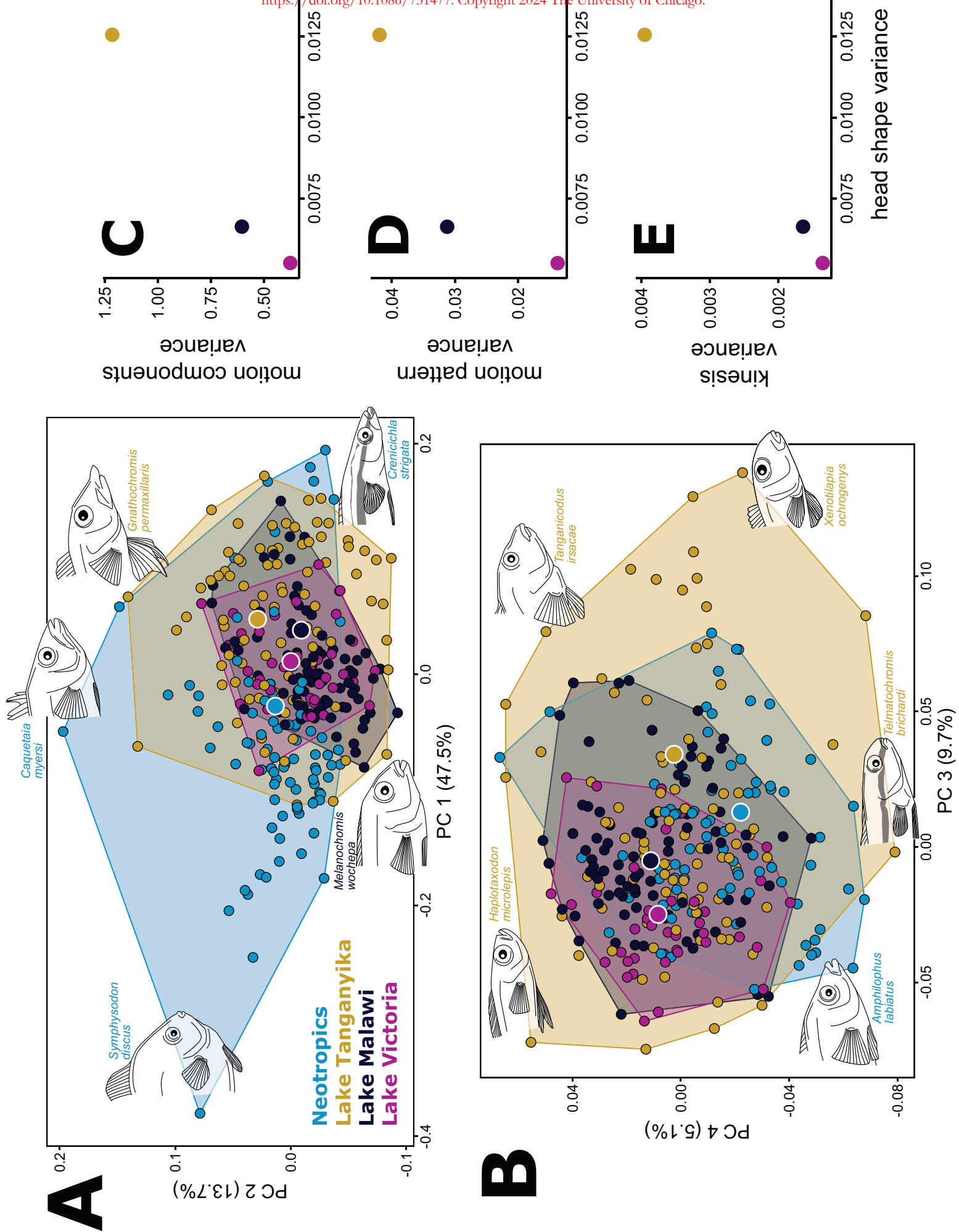


Figure 5

This is the author's accepted manuscript without copyediting, formatting, or final corrections. It will be published in its final form in an upcoming issue of The American Naturalist, published by The University of Chicago Press. Include the DOI when citing or quoting:
<https://doi.org/10.1086/731477>. Copyright 2024 The University of Chicago.



Supplement to
Replicated Functional Evolution in Cichlid Adaptive Radiations

Christopher M. Martinez^{1,*,**}, Katherine A. Corn^{2,3,4, *,**}, Sarah Williamson², Darien Satterfield²,
Alexus S. Roberts-Hugghis², Anthony Barley⁴, Samuel R. Borstein⁶, Matthew D. McGee⁷, and
Peter C. Wainwright²

¹Department of Ecology and Evolutionary Biology, University of California, Irvine, 92697, USA

²Department of Evolution and Ecology, University of California, Davis, 95616, USA

³Department of Biological Sciences, Virginia Polytechnic Institute and State University,
Blacksburg, VA, 24061, USA

⁴School of Biological Sciences, Washington State University, Pullman, WA, 99163, USA

⁵School of Mathematical and Natural Sciences, Arizona State University–West Campus,
Glendale, AZ, 85306, USA

⁶Department of Ecology and Evolutionary Biology, University of Michigan, Ann Arbor, MI,
USA

⁷School of Biological Sciences, Monash University, Melbourne, Victoria, Australia

*Correspondence: c.martinez@uci.edu (C.M.M); cornkatherineap@gmail.com (K.A.C)

**Authors contributed equally to this paper.

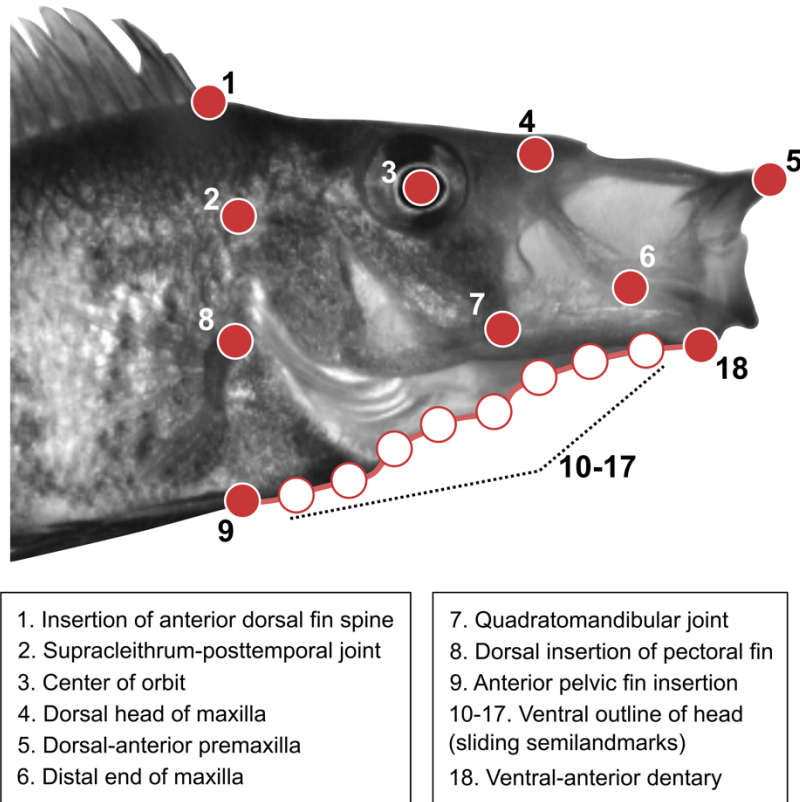


Figure S1. Cranial landmarks used to capture feeding kinematics in this study. 10 fixed landmarks are shown as red dots with a white border, and 8 sliding semilandmarks are included in white with a red border.

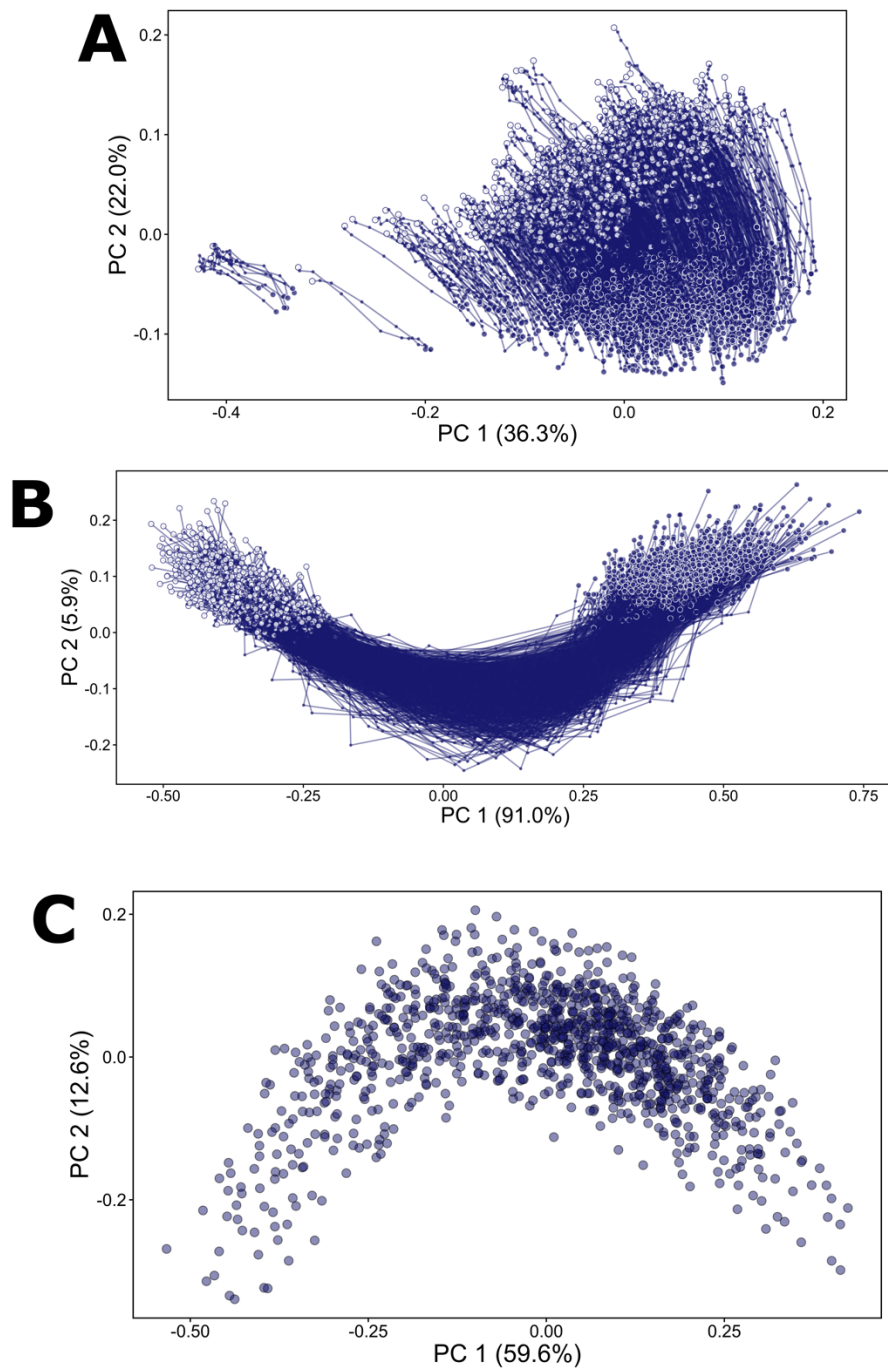


Figure S2. Process of alignment of shape trajectory data for the motion pattern trait. **A)** PCs 1 and 2 for aligned motion shapes representing 1,110 suction feeding events. Each line is a trajectory for a single feeding motion. The subjects of alignment (and scaling) are individual cranial shapes at different stages of a motion. **B)** Trajectory shapes shown in panel A are scaled and aligned. Here, the subject of alignment is the entire collection of 10 cranial shapes for a motion. **C)** Each of the 1,110 trajectory shapes is plotted as a single point in morphospace. Points closer to each other have more similar motion patterns than more distantly spaced points.

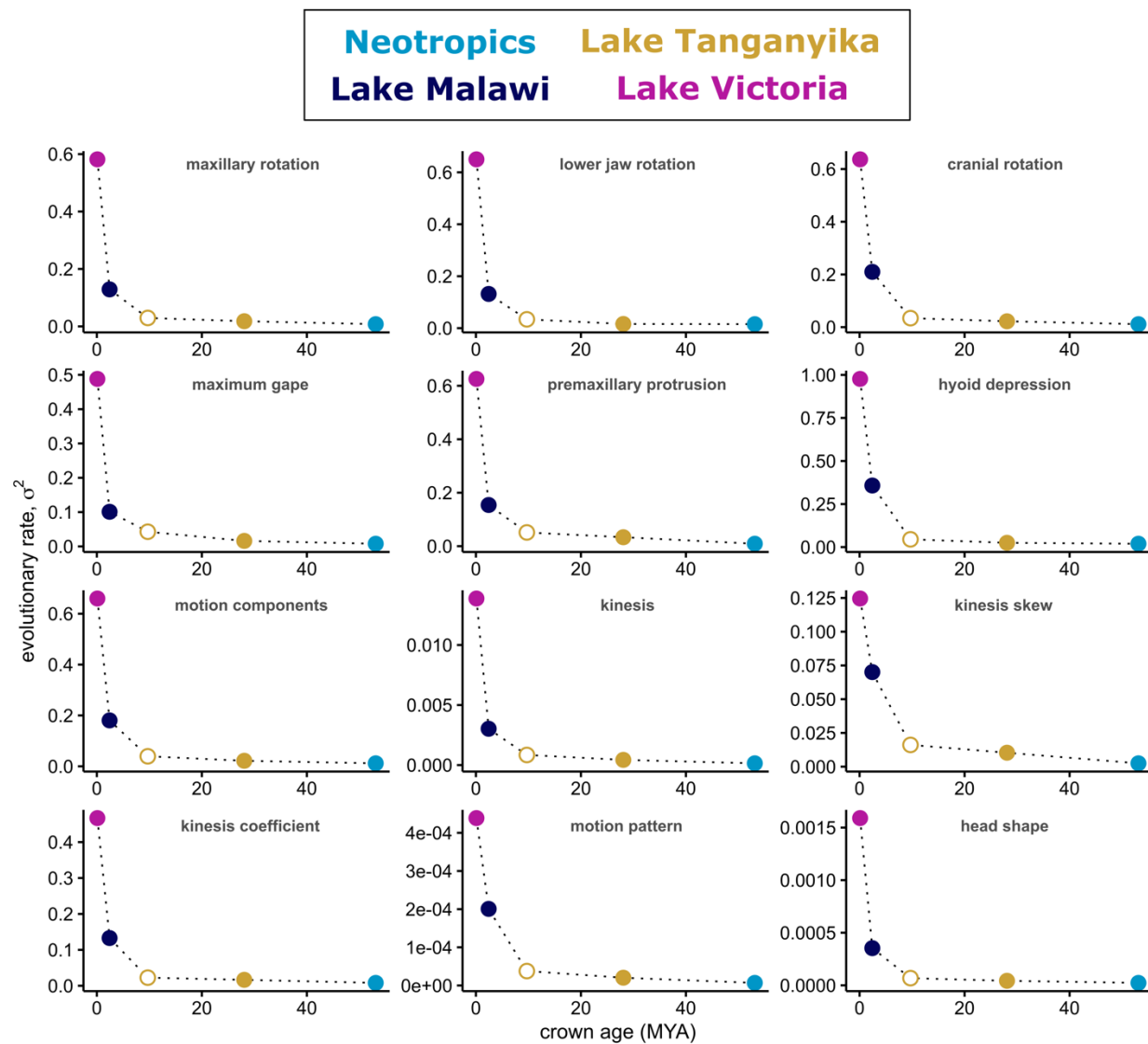


Figure S3. Rates of trait evolution versus radiation age. Estimated Brownian rate parameters for functional and morphological traits plotted against radiation crown age. Relative rates among radiations were highly consistent for all traits, all showing negative trends with radiation age. Rates for all radiations were estimated with a tree from McGee et al. (2020). In addition, rates for Lake Tanganyika were estimated with a tree from Ronco et al. (2021), as it reconstructs an earlier radiation age (white dot with yellow border). The rank order of rates was the same for either Lake Tanganyika estimate, as was the negative temporal trend across radiations.

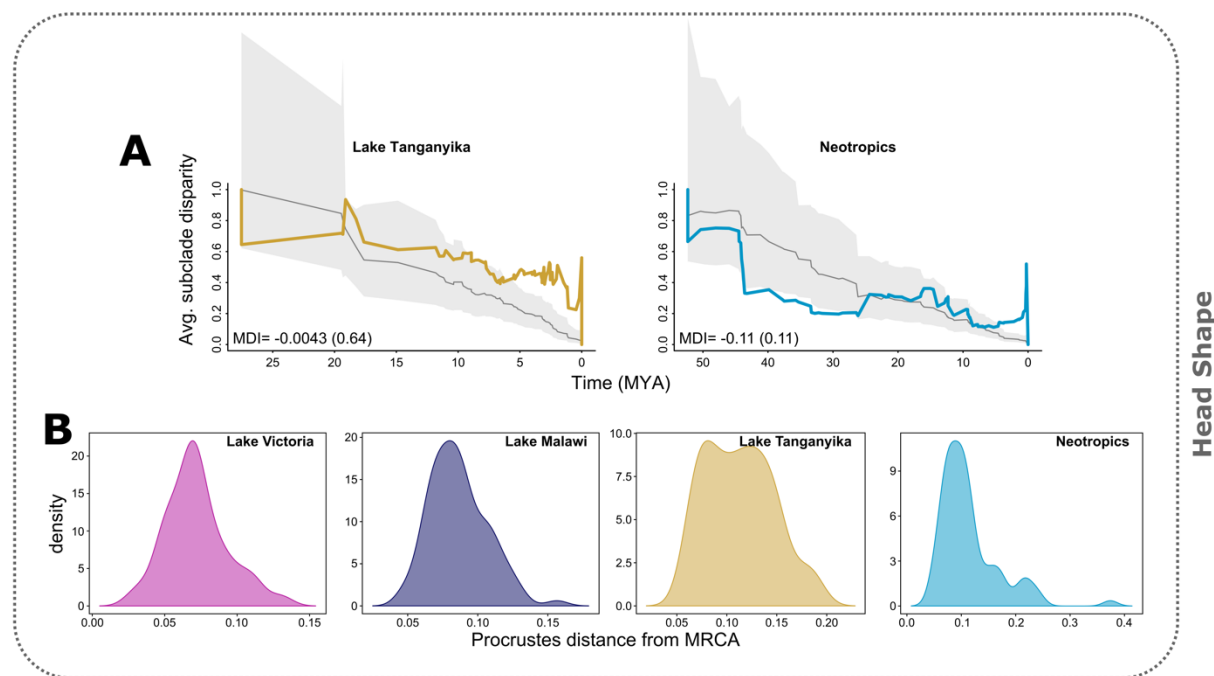


Figure S4. Evolution of head shape in cichlids. Disparity through time (DTT) plots for A) head shape in the two oldest cichlid radiations, Lake Tanganyika and the Neotropics. Also shown are B) distributions of Procrustes distances of head shapes between extant species and their most recent common ancestors (MRCA).

Table S1. Cichlid species examined in this study. 300 species are listed and colored by radiation. The number of individual fish per species is provided in parentheses. On average, there were 3.1 (+/- 0.58 SD) feeding motions per individual fish. Asterisks denote species from Martinez et al. 2018. All other species represent new data to this study.

LAKE VICTORIA	<i>Yssichromis</i> sp. 'tipped blue' (1)	<i>Lethrinops marginatus</i> (1)
<i>Enterochromis paropius</i> (1)		<i>Maylandia elegans</i> (1)
<i>Haplochromis chilotes</i> (2)		<i>Maylandia lombardoi</i> (1)
<i>Haplochromis howesi</i> (1)	<i>Aulonocara aquilonium</i> (1)	<i>Maylandia mbenjii</i> (1)
<i>Haplochromis lividus</i> (1)	<i>Aulonocara gertrudae</i> (1)	<i>Maylandia nigrodorsalis</i> (1)
<i>Haplochromis</i> sp. 'blue obliquidens' (1)	<i>Aulonocara jacobfreibergi</i> (1)	<i>Mchenga conophoros</i> (1)
<i>Haplochromis</i> sp. 'Murchison Bay' (1)	<i>Aulonocara koningsi</i> (1)	<i>Melanochromis auratus</i> (1)*
<i>Haplochromis</i> sp. 'thickskin' (1)	<i>Aulonocara maylandi</i> (1)	<i>Melanochromis baliodigma</i> (1)
<i>Haplochromis thereuterion</i> (1)	<i>Aulonocara rostratum</i> (1)	<i>Melanochromis kaskazini</i> (1)*
<i>Haplochromis vonlinnei</i> (1)	<i>Aulonocara stuartgranti</i> (1)*	<i>Melanochromis loriae</i> (1)
<i>Harpagochromis</i> cf. <i>squamulatus</i> (1)	<i>Buccochromis nototaenia</i> (1)	<i>Melanochromis vermiculus</i> (1)
<i>Harpagochromis</i> sp. 'golden duck' (1)	<i>Buccochromis rhoadesii</i> (1)	<i>Melanochromis wochepa</i> (1)
<i>Labrochromis ishmaeli</i> (1)	<i>Buccochromis spectabilis</i> (1)	<i>Mylochromis anaphyrmus</i> (1)
<i>Lipochromis melanopterus</i> (1)	<i>Caprichromis liemi</i> (1)	<i>Mylochromis ericotaenia</i> (1)
<i>Lipochromis parvidens</i> (1)	<i>Champsochromis caeruleus</i> (1)	<i>Mylochromis sphaerodon</i> (1)
<i>Lipochromis</i> sp. 'matumbi hunter' (1)	<i>Champsochromis spilorhynchus</i> (1)	<i>Naevochromis chrysogaster</i> (1)
<i>Lithochromis rubripinnis</i> (1)	<i>Cheilochromis euchilus</i> (1)*	<i>Nimbochromis fuscotaeniatus</i> (1)
<i>Mbipia lutea</i> (1)	<i>Chilotilapia rhoadesii</i> (1)*	<i>Nimbochromis linni</i> (1)
<i>Neochromis greenwoodi</i> (1)	<i>Chindongo demasoni</i> (1)	<i>Nimbochromis polystigma</i> (1)*
<i>Neochromis nigricans</i> (1)	<i>Chindongo flavus</i> (1)*	<i>Nimbochromis venustus</i> (1)
<i>Neochromis omnicaeruleus</i> (1)	<i>Chindongo socolofi</i> (1)	<i>Nyassachromis boadzulu</i> (1)
<i>Neochromis rufocaudalis</i> (1)	<i>Copadichromis azureus</i> (1)	<i>Otopharynx antron</i> (1)
<i>Neochromis</i> sp. 'Bihiru scraper' (1)	<i>Copadichromis borleyi</i> (3)	<i>Otopharynx lithobates</i> (1)*
<i>Paralabidochromis chromogynos</i> (1)	<i>Copadichromis chrysonotus</i> (3)	<i>Otopharynx tetrastigma</i> (1)
<i>Paralabidochromis sauvagei</i> (1)	<i>Copadichromis geertsii</i> (1)	<i>Petrotilapia micragalana</i> (1)
<i>Platytaeniodus</i> sp. 'red tail sheller' (1)	<i>Copadichromis melas</i> (1)	<i>Placidochromis electra</i> (1)*
<i>Prognathochromis perrieri</i> (1)	<i>Copadichromis trewavasae</i> (1)	<i>Placidochromis johnstoni</i> (1)
<i>Ptyochromis fischeri</i> (1)	<i>Copadichromis virginalis</i> (1)	<i>Placidochromis milomo</i> (2)*
<i>Ptyochromis</i> sp. 'red rock sheller' (1)	<i>Ctenopharynx nitidus</i> (1)	<i>Placidochromis phenochilus</i> (1)
<i>Ptyochromis</i> sp. 'salmon' (1)	<i>Cynotilapia axelrodi</i> (1)	<i>Protomelas dejunctus</i> (1)
<i>Pundamilia macrocephala</i> (1)	<i>Cynotilapia zebroides</i> (1)	<i>Protomelas fenestratus</i> (1)
<i>Pundamilia nyererei</i> (1)	<i>Cyrtocara moorii</i> (1)	<i>Protomelas labridens</i> (1)
<i>Pundamilia pundamilia</i> (1)	<i>Dimidiochromis compressiceps</i> (1)	<i>Protomelas marginatus</i> (1)
<i>Pundamilia</i> sp. 'crimson tide' (1)	<i>Dimidiochromis kiwinge</i> (1)	<i>Protomelas spilonotus</i> (1)
<i>Pundamilia</i> sp. 'pink anal' (1)	<i>Fossorochromis rostratus</i> (1)*	<i>Protomelas spilopterus</i> (1)
<i>Pundamilia</i> sp. 'red flank' (1)	<i>Iodotropheus sprengerae</i> (1)	<i>Protomelas taeniolatus</i> (1)
<i>Pundamilia</i> sp. 'red head' (1)	<i>Labeotropheus fuelleborni</i> (2)*	<i>Pseudotropheus crabro</i> (1)*
<i>Pyxichromis orthostoma</i> (1)	<i>Labeotropheus trewavasae</i> (2)*	<i>Pseudotropheus cyaneorhabdos</i> (1)
<i>Xystichromis phytophagus</i> (1)	<i>Labidochromis caeruleus</i> (2)	<i>Pseudotropheus galanos</i> (1)
<i>Yssichromis piceatus</i> (1)	<i>Labidochromis joanjohnsonae</i> (1)	<i>Pseudotropheus interruptus</i> (1)

Table S1. List of cichlid species, continued.

<i>Pseudotropheus johannii</i> (1)	<i>Lamprologus speciosus</i> (1)	<i>Trematochromis benthicola</i> (2)*
<i>Rhamphochromis ferox</i> (1)	<i>Lepidiolamprologus attenuatus</i> (3)*	<i>Triglachromis otostigma</i> (1)
<i>Rhamphochromis longiceps</i> (1)*	<i>Lepidiolamprologus elongatus</i> (1)	<i>Tropheus brichardi</i> (1)
<i>Sciaenochromis fryeri</i> (1)	<i>Lepidiolamprologus nkambae</i> (1)	<i>Tropheus duboisi</i> (1)
<i>Stigmatochromis modestus</i> (1)	<i>Limnochromis auritus</i> (2)*	<i>Tropheus moorii</i> (1)
<i>Taeniolethrinops laticeps</i> (1)	<i>Limnotilapia dardennii</i> (1)	<i>Variabilichromis moorii</i> (2)*
<i>Tropheops romandi</i> (1)	<i>Lobochilotes labiatus</i> (1)	<i>Xenotilapia leptura</i> (1)
<i>Tyrannochromis nigriventer</i> (1)	<i>Neolamprologus boulengeri</i> (2)*	<i>Xenotilapia melanogenys</i> (1)
LAKE TANGANYIKA	<i>Neolamprologus cylindricus</i> (1)*	<i>Xenotilapia ochrogenys</i> (1)
<i>Altolamprologus calvus</i> (1)	<i>Neolamprologus fasciatus</i> (1)*	<i>Xenotilapia ornatipinnis</i> (1)
<i>Altolamprologus compressiceps</i> (1)	<i>Neolamprologus furcifer</i> (2)*	<i>Xenotilapia papilio</i> (1)
<i>Astatotilapia burtoni</i> (1)*	<i>Neolamprologus hecqui</i> (1)*	<i>Xenotilapia rotundiventralis</i> (1)
<i>Astatotilapia stappersii</i> (1)	<i>Neolamprologus longicaudatus</i> (3)*	NEOTROPICS
<i>Aulonocranus dewindti</i> (1)	<i>Neolamprologus longior</i> (3)*	<i>Acarichthys heckelii</i> (1)
<i>Bathybates minor</i> (1)*	<i>Neolamprologus meeli</i> (3)*	<i>Acaronia nassa</i> (1)
<i>Boulengerochromis microlepis</i> (3)	<i>Neolamprologus modestus</i> (1)*	<i>Aequidens diadema</i> (1)
<i>Callochromis macrops</i> (1)	<i>Neolamprologus mondabu</i> (1)	<i>Aequidens metae</i> (2)
<i>Callochromis pleurospilus</i> (1)	<i>Neolamprologus multifasciatus</i> (1)	<i>Aequidens tetramerus</i> (1)
<i>Cardiopharynx schoutedeni</i> (1)	<i>Neolamprologus nigriventris</i> (1)*	<i>Amatitlania kanna</i> (1)
<i>Chalinochromis brichardi</i> (1)*	<i>Neolamprologus obscurus</i> (4)*	<i>Amatitlania myrnae</i> (1)
<i>Chalinochromis popelini</i> (1)	<i>Neolamprologus prochilus</i> (4)*	<i>Amatitlania nanolutea</i> (1)
<i>Ctenochromis horei</i> (1)	<i>Neolamprologus pulcher</i> (1)*	<i>Amatitlania nigrofasciata</i> (1)
<i>Cyphotilapia frontosa</i> (1)	<i>Neolamprologus savoryi</i> (3)*	<i>Amatitlania sajica</i> (2)
<i>Cyprichromis coloratus</i> (1)	<i>Neolamprologus sexfasciatus</i> (2)*	<i>Amatitlania septemfasciata</i> (1)
<i>Cyprichromis leptosoma</i> (1)	<i>Neolamprologus similis</i> (1)	<i>Amatitlania siquia</i> (1)
<i>Cyprichromis microlepidotus</i> (1)	<i>Neolamprologus tetracanthus</i> (1)*	<i>Amphilophus citrinellus</i> (1)
<i>Cyprichromis pavo</i> (1)*	<i>Neolamprologus walteri</i> (1)*	<i>Amphilophus labiatus</i> (1)
<i>Cyprichromis zonatus</i> (1)	<i>Ophthalmotilapia boops</i> (1)*	<i>Amphilophus sagittae</i> (1)
<i>Ectodus descampsii</i> (1)*	<i>Ophthalmotilapia nasuta</i> (3)*	<i>Amphilophus trimaculatus</i> (1)
<i>Eretmodus cyanostictus</i> (1)*	<i>Paracyprichromis brieni</i> (1)	<i>Andinoacara stalsbergi</i> (1)
<i>Gnathochromis permaxillaris</i> (1)*	<i>Paracyprichromis nigripinnis</i> (1)	<i>Archocentrus centrarchus</i> (1)
<i>Gnathochromis pfefferi</i> (1)	<i>Perissodus microlepis</i> (2)	<i>Astronotus ocellatus</i> (1)
<i>Grammatotria lemairei</i> (1)	<i>Petrochromis orthognathus</i> (1)	<i>Australoheros scitulus</i> (1)
<i>Greenwoodochromis bellcrossi</i> (1)	<i>Pseudosimochromis babaulti</i> (1)*	<i>Biotodoma cupido</i> (1)
<i>Haplotaxodon microlepis</i> (1)*	<i>Pseudosimochromis curvifrons</i> (1)	<i>Biotodoma wavrini</i> (1)
<i>Interochromis loocki</i> (1)	<i>Reganochromis calliurus</i> (1)	<i>Caquetaia kraussii</i> (1)
<i>Julidochromis dickfeldi</i> (1)*	<i>Spathodus erythrodon</i> (1)	<i>Caquetaia myersi</i> (3)
<i>Julidochromis marlieri</i> (1)	<i>Tanganicodus irsacae</i> (1)	<i>Caquetaia spectabilis</i> (1)
<i>Julidochromis ornatus</i> (1)	<i>Telmatochromis brichardi</i> (1)	<i>Chaetobranchus flavescens</i> (1)
<i>Lamprologus callipterus</i> (1)*	<i>Telmatochromis dhonti</i> (1)*	<i>Chiapaheros grammodes</i> (1)
<i>Lamprologus lemairii</i> (3)*	<i>Telmatochromis temporalis</i> (2)*	<i>Cichla ocellaris</i> (1)
<i>Lamprologus ornatipinnis</i> (1)	<i>Telmatochromis vittatus</i> (1)	<i>Cichlasoma dimerus</i> (1)
<i>Lamprologus signatus</i> (1)	<i>Trematocara variabile</i> (3)	<i>Cincelichthys bocourti</i> (1)

Table S1. List of cichlid species, continued.

<i>Cleithracara maronii</i> (1)	<i>Heroina isonycterina</i> (1)	<i>Parachromis dovii</i> (1)
<i>Crenicara punctulatum</i> (1)	<i>Heros severus</i> (2)	<i>Parachromis managuensis</i> (1)
<i>Crenicichla lepidota</i> (1)	<i>Herotilapia multispinosa</i> (1)	<i>Paraneetroplus gibbiceps</i> (1)
<i>Crenicichla regani</i> (1)	<i>Hoplarchus psittacus</i> (1)	<i>Petenia splendida</i> (1)
<i>Crenicichla saxatilis</i> (1)	<i>Hypselecara coryphaenoides</i> (1)	<i>Pterophyllum scalare</i> (3)
<i>Crenicichla strigata</i> (1)	<i>Hypselecara temporalis</i> (1)	<i>Retroculus lapidifer</i> (1)
<i>Crenicichla sveni</i> (1)	<i>Hypsophrys nematopus</i> (1)	<i>Rocio octofasciata</i> (1)
<i>Cribroheros robertsoni</i> (1)	<i>Krobia xinguensis</i> (1)	<i>Satanoperca daemon</i> (1)
<i>Cryptoheros spilurus</i> (1)	<i>Kronoheros umbrifer</i> (1)	<i>Sympodus discus</i> (3)
<i>Dicrossus maculatus</i> (1)	<i>Laetacara araguaiae</i> (1)	<i>Tahuantinsuyoa macantzatza</i> (1)
<i>Geophagus abalios</i> (1)	<i>Laetacara thayeri</i> (1)	<i>Talamancatheros sieboldii</i> (1)
<i>Geophagus crassilabris</i> (1)	<i>Maskaheros argenteus</i> (1)	<i>Teleocichla centrarchus</i> (1)
<i>Geophagus iporangensis</i> (1)	<i>Mayaheros urophthalmus</i> (3)	<i>Trichromis salvini</i> (3)
<i>Geophagus megasema</i> (1)	<i>Mesoheros festae</i> (1)	<i>Uaru amphiacanthoides</i> (1)
<i>Geophagus parnaibae</i> (1)	<i>Mesonauta mirificus</i> (1)	<i>Vieja breidohri</i> (1)
<i>Geophagus steindachneri</i> (1)	<i>Mikrogeophagus ramirezi</i> (1)	<i>Vieja fenestrata</i> (2)
<i>Geophagus winemilleri</i> (1)	<i>Nandopsis tetracanthus</i> (2)	<i>Vieja synspila</i> (1)
<i>Guianacara stergiosi</i> (1)	<i>Nosferatu pantostictus</i> (1)	
<i>Gymnogeophagus tiraparae</i> (1)	<i>Panamius panamensis</i> (1)	

Table S2. Phylogenetic placement of undescribed Lake Victoria cichlids. Correspondence of undescribed species from this study with the tree tips used from a published phylogeny (McGee et al. 2020). Sources of supporting literature for placements are also provided. See supplemental methods for additional procedural details.

This Study	McGee et al. (2020) Phylogeny	Source
<i>Haplochromis</i> sp. 'blue obliquidens'	<i>Haplochromis obliquidens</i>	Seehausen (1996)
<i>Haplochromis</i> sp. 'Murchison Bay'	<i>Haplochromis riponianus</i>	Greenwood (1980)
<i>Haplochromis</i> sp. 'thickskin'	<i>Haplochromis plagiodon</i>	McGee et al. (2020)
<i>Harpagochromis</i> sp. 'golden duck'	<i>Haplochromis prognathus</i>	Greenwood (1980)
<i>Lipochromis</i> sp. 'matumbi hunter'	<i>Haplochromis obesus</i>	Seehausen (1996)
<i>Neochromis</i> sp. 'Bihiru scraper'	<i>Neochromis simotes</i>	Seehausen (1996)
<i>Platytaeniodus</i> sp. 'red tail sheller'	<i>Haplochromis xenognathus</i>	Greenwood (1980)
<i>Ptyochromis</i> sp. 'red rock sheller'	<i>Haplochromis granti</i>	Greenwood (1980)
<i>Ptyochromis</i> sp. 'salmon'	<i>Haplochromis prodromus</i>	Greenwood (1980)
<i>Pundamilia</i> sp. 'crimson tide'	<i>Pundamilia igneopinnis</i>	Seehausen et al. (1998)
<i>Pundamilia</i> sp. 'pink anal'	<i>Mbipia mbipi</i>	McGee et al. (2020)
<i>Pundamilia</i> sp. 'red flank'	<i>Haplochromis parorthostoma</i>	Seehausen (1996)
<i>Pundamilia</i> sp. 'red head'	<i>Haplochromis pallidus</i>	Seehausen (1996)
<i>Yssichromis</i> sp. 'tipped blue'	<i>Haplochromis pyrrhocephalus</i>	Greenwood (1980)

TABLE S3. Comparisons of variances for functional traits and head shape. Variances are shown on the left and P-values from pairwise comparisons are on the right. Statistically significant results are shown in bold, and are based on 10,000 permutations

Trait	Variances				Pairwise P-values					
	Vic	Mal	Tan	Neo	Mal - Neo	Mal - Tan	Mal - Vic	Neo - Tan	Neo - Vic	Tan - Vic
motion components	0.38	0.60	1.22	1.10	0.00040	0.00010	0.21	0.43	0.00010	0.00010
motion pattern	0.014	0.031	0.042	0.033	0.82	0.064	0.016	0.10	0.0094	0.00040
premaxillary protrusion	0.058	0.11	0.27	0.17	0.14	0.00010	0.30	0.017	0.029	0.00020
maxillary rotation	0.056	0.066	0.15	0.090	0.34	0.00050	0.74	0.012	0.27	0.0022
lower jaw rotation	0.065	0.074	0.17	0.15	0.0070	0.00070	0.82	0.43	0.019	0.0030
cranial rotation	0.058	0.10	0.20	0.27	0.00020	0.032	0.46	0.15	0.00060	0.017
hyoid depression	0.091	0.20	0.29	0.34	0.0054	0.091	0.098	0.26	0.00030	0.0034
mouth gape	0.047	0.051	0.14	0.084	0.33	0.0020	0.91	0.080	0.35	0.022
kinesis	0.0014	0.0016	0.0040	0.0021	0.44	0.00010	0.70	0.0007	0.31	0.00080
log-kinesis skew	0.011	0.030	0.047	0.036	0.49	0.034	0.055	0.16	0.011	0.00050
log-kinesis coefficient	0.043	0.061	0.12	0.17	0.0003	0.055	0.65	0.15	0.0022	0.046
head shape	0.0055	0.0066	0.013	0.015	0.00010	0.00060	0.63	0.25	0.00020	0.0022

Vic= Lake Victoria; Mal= Lake Malawi; Tan= Lake Tanganyika; Neo=Neotropics

Table S4. Hypervolume results for functional and morphological traits. Each row contains a comparison between two radiations or between one radiation and all other species. The column to the right displays results of a randomization procedure that compared fractions of unique hypervolume spaces between cichlid radiations. Percentiles display how extreme observed results are relative to 10,000 randomized permutations.

Trait	Hypervolume 1 (H1)	Hypervolume 2 (H2)	Volume (H1, H2)	Sorenson overlap	Unique fraction (H1, H2)	Percentile from Randomization: Unique fraction (H1, H2)
components	Tanganyika	Non-Tanganyika	(14.93, 7.00)	0.52	(0.62, 0.19)	(0.999, 0.096)
components	Neotropics	Non-Neotropics	(9.50, 7.87)	0.56	(0.49, 0.39)	(0.995, 0.797)
components	Malawi	Non-Malawi	(3.74, 12.51)	0.43	(0.06, 0.72)	(0.000, 0.999)
components	Victoria	Non-Victoria	(1.77, 11.34)	0.26	(0.03, 0.85)	(0.000, 0.999)
components	Tanganyika	Neotropics	(14.93, 9.50)	0.51	(0.58, 0.35)	(0.996, 0.695)
components	Tanganyika	Malawi	(14.93, 3.74)	0.37	(0.77, 0.08)	(0.999, 0.001)
components	Tanganyika	Victoria	(14.93, 1.77)	0.21	(0.88, 0.01)	(0.999, 0.999)
components	Malawi	Victoria	(3.74, 1.77)	0.53	(0.61, 0.17)	(0.971, 0.117)
components	Malawi	Neotropics	(3.74, 9.50)	0.44	(0.23, 0.69)	(0.232, 0.999)
components	Victoria	Neotropics	(1.77, 9.50)	0.25	(0.22, 0.85)	(0.257, 0.999)
motion pattern	Tanganyika	Non-Tanganyika	(0.0078, 0.0038)	0.62	(0.54, 0.050)	(0.997, 0.001)
motion pattern	Neotropics	Non-Neotropics	(0.0047, 0.0047)	0.74	(0.26, 0.26)	(0.632, 0.595)
motion pattern	Malawi	Non-Malawi	(0.0042, 0.0052)	0.78	(0.14, 0.30)	(0.151, 0.707)
motion pattern	Victoria	Non-Victoria	(0.0013, 0.0055)	0.38	(0.010, 0.76)	(0.999, 0.999)
motion pattern	Tanganyika	Neotropics	(0.0078, 0.0047)	0.66	(0.47, 0.12)	(0.941, 0.080)
motion pattern	Tanganyika	Malawi	(0.0078, 0.0042)	0.66	(0.49, 0.060)	(0.960, 0.004)
motion pattern	Tanganyika	Victoria	(0.0078, 0.0013)	0.29	(0.83, 0.010)	(0.999, 0.999)
motion pattern	Malawi	Victoria	(0.0042, 0.0013)	0.47	(0.69, 0.030)	(0.996, 0.001)
motion pattern	Malawi	Neotropics	(0.0042, 0.0047)	0.73	(0.22, 0.31)	(0.422, 0.659)
motion pattern	Victoria	Neotropics	(0.0013, 0.0047)	0.42	(0.040, 0.73)	(0.004, 0.998)
head shape	Tanganyika	Non-Tanganyika	(0.0014, 0.00088)	0.53	(0.57, 0.3)	(0.999, 0.672)
head shape	Neotropics	Non-Neotropics	(0.0011, 0.00083)	0.46	(0.59, 0.47)	(0.999, 0.982)
head shape	Malawi	Non-Malawi	(0.00033, 0.0016)	0.33	(0.05, 0.8)	(0.000, 0.999)
head shape	Victoria	Non-Victoria	(0.00022, 0.0014)	0.27	(0.03, 0.84)	(0.000, 0.999)
head shape	Tanganyika	Neotropics	(0.0014, 0.0011)	0.44	(0.62, 0.48)	(0.999, 0.976)
head shape	Tanganyika	Malawi	(0.0014, 0.00033)	0.33	(0.8, 0.13)	(0.999, 0.041)
head shape	Tanganyika	Victoria	(0.0014, 0.00022)	0.25	(0.86, 0.08)	(0.999, 0.013)
head shape	Malawi	Victoria	(0.00033, 0.00022)	0.62	(0.49, 0.23)	(0.898, 0.385)
head shape	Malawi	Neotropics	(0.00033, 0.0011)	0.33	(0.3, 0.78)	(0.648, 0.999)
head shape	Victoria	Neotropics	(0.00022, 0.0011)	0.26	(0.26, 0.84)	(0.483, 0.999)

TABLE S5. Comparisons of evolutionary rates for functional traits and head shape. Rates are shown on the left and P-values from pairwise comparisons are on the right. Statistically significant results are shown in bold, and are based on 10,000 permutations. Rates were computed using the McGee et al. (2020) tree for all radiations, as well as with a tree from Ronco et al. (2021) for Lake Tanganyika only (column labeled Tan-R). Pairwise comparisons were only made for the former.

Trait	Brownian rate parameter					Pairwise P-values					
	Vic	Mal	Tan	Tan-R	Neo	Mal - Neo	Mal - Tan	Mal - Vic	Neo - Tan	Neo - Vic	Tan - Vic
motion components	0.66	0.18	0.022	0.039	0.012	0.00020	0.00015	0.0012	0.046	0.00010	0.00010
motion pattern	0.00044	0.00020	0.000020	0.000038	0.0000068	0.00020	0.00010	0.040	0.00040	0.00010	0.00010
premaxillary protrusion	0.63	0.15	0.033	0.051	0.0091	0.00020	0.00090	0.021	0.0060	0.00020	0.00020
maxillary rotation	0.58	0.13	0.018	0.029	0.0079	0.00020	0.00020	0.010	0.076	0.00020	0.00015
lower jaw rotation	0.65	0.13	0.016	0.034	0.015	0.00020	0.00015	0.0084	0.96	0.00020	0.00010
cranial rotation	0.64	0.21	0.022	0.034	0.011	0.00020	0.00020	0.040	0.13	0.00010	0.00010
hyoid depression	0.98	0.36	0.025	0.045	0.020	0.00020	0.00020	0.054	0.57	0.00010	0.00010
mouth gape	0.49	0.10	0.016	0.043	0.0078	0.00010	0.00010	0.0057	0.12	0.00010	0.00010
kinesis	0.014	0.0030	0.00043	0.00084	0.00015	0.00020	0.00010	0.0062	0.017	0.00015	0.00010
log-kinesis skew	0.12	0.070	0.010	0.016	0.0025	0.00010	0.00010	0.21	0.00015	0.00020	0.00020
log-kinesis coefficient	0.47	0.13	0.017	0.023	0.0080	0.00020	0.00015	0.027	0.11	0.00020	0.00020
head shape	0.0016	0.00035	0.000043	0.000068	0.000023	0.00020	0.00015	0.00020	0.03	0.00010	0.00010

Vic= Lake Victoria; Mal= Lake Malawi; Tan & Tan-R= Lake Tanganyika; Neo=Neotropics

Table S6. Results from Disparity Though Time (DTT) analyses. Morphological Disparity Index (MDI) values are reported, describing the deviation of subclade trait disparities from simulated values under Brownian motion. P-values shown in parentheses. Note that none of the results are statistically significant, meaning that trait diversification was statistically consistent with a Brownian process.

Trait	All Species	Victoria	Malawi	Tanganyika	Neotropics
motion components	0.029 (0.72)	-0.012 (0.37)	0.15 (0.92)	0.0088 (0.61)	0.019 (0.69)
motion pattern	0.096 (0.88)	0.12 (0.84)	0.40 (0.99)	0.30 (0.98)	0.16 (0.94)
head shape	-0.083 (0.40)	-0.080 (0.067)	0.092 (0.84)	-0.0043 (0.64)	-0.11 (0.11)

Supplementary Information

Materials & Methods

Phylogeny matching – For comparative analyses, species were matched to a phylogeny of cichlids by McGee and colleagues (McGee et al. 2020). This phylogeny is limited to only described cichlid species. Several cichlids from Lake Victoria in our dataset (n=14 species) are currently known in the literature but remain undescribed (e.g., *Pundamilia* sp. ‘red flank’). We used existing phylogenomic and systematic knowledge to assign undescribed taxa to Lake Victoria cichlid species in the phylogeny with which they share key diagnostic features or previous molecular studies have suggested may be close relatives (Table S2; Greenwood 1980; Seehausen 1996; Seehausen et al. 1998; McGee et al. 2020).

Maximum ages of cichlid radiations – There is considerable interest in the age of cichlids and of major clades within this group. Possible ages of the two youngest radiations in this study, Lakes Malawi and Victoria, have traditionally been bounded by geological events. Lake Malawi is reported to have almost completely desiccated between 1.6-1 Ma (Delvaux 1995). Additionally, Lake Victoria cichlids are thought to have radiated within the last 150,000 years (Verheyen et al. 2003; Meier et al. 2017), although evidence exists for large-scale (and possibly complete) desiccation of the lake as recently as 18,000-10,000 years ago (Johnson et al. 1996, Stager and Johnson 2008). For the Lake Tanganyika radiation, whole-genome fossil-calibrated assessments place the age of the *in-situ* radiation at around 10 Ma (Matschiner et al. 2020; Ronco et al. 2021), reducing the age from previous estimates between 30-20 Ma (e.g., McGee et al. 2020). Additionally, there has been much debate and uncertainty surrounding the timing of the split between the subfamily Cichlinae (Neotropical cichlids) and Pseudocrenilabrinae (African

cichlids), and by extension, the crown ages of these large clades. Some earlier molecular-based phylogenetic reconstructions resulted in topologies that appeared congruent with the splitting of landmasses during Gondwanan vicariance, which would place divergence of current day Neotropical and African subfamilies at 120-100 Ma (Sparks 2004; Sparks and Smith 2004). However, several recent studies favor a trans-Atlantic dispersal model of cichlid phylogeography, with several estimates between 70-45 Ma (Matschiner 2018). Moreover, an even more recent study using whole genomes and fossil calibration places the divergence of Cichlinae and Pseudocrenilabrinae at approximately 62 Ma (Matschiner et al. 2020).

The phylogeny used in this study was trimmed from a previously published tree (McGee et al. 2020), although displaying some differences from ages listed above, preserves a rank order of radiation ages that is consistent with recent phylogenetic reconstructions of cichlids; with an estimated 53.1 Ma for the Neotropics, 28.1 Ma for Lake Tanganyika, 2.4 Ma for Lake Malawi, and 0.1 Ma for Lake Victoria. While the accepted timing of cichlid evolution can (and certainly will) change with new data, short of a major upheaval in the estimates of divergence times, the rank order of ages is unlikely to be upturned. Therefore, rates of trait evolution examined in our study, which depend on inferred timing from a phylogeny, may similarly change, but overall interpretations of functional diversification across radiations differing in their relative time scales (tens of millions of years to thousands of years) are expected to remain largely intact.

Literature Cited

- Delvaux, D. 1995. Age of Lake Malawi (Nyasa) and water level fluctuations. Musée Royal Afrique Centrale, Tervuren (Belgique), Department de Géologie et Mineralogies, Rapport Annuel 1995-1996:99-108.
- Greenwood, P. H. 1980. Towards a phyletic classification of the 'genus' *Haplochromis* (Pisces, Cichlidae) and related taxa. Part 2; the species from Lakes Victoria, Nabugabo, Edward, George and Kivu. Bulletin of the British Museum (Natural History) Zoology. 39:1-101.
- Johnson, T. C., C. A. Scholz, M. R. Talbot, K. Kelts, R. D. Ricketts, G. Ngobi, K. Beuning, I. Ssemmanda, and J. W. McGill. 1996. Late Pleistocene desiccation of Lake Victoria and rapid evolution of cichlid fishes. Science 273:1091-1093.
- Matschiner, M. 2018. Gondwanan vicariance or trans-Atlantic dispersal of cichlid fishes: a review of the molecular evidence. Hydrobiologia 832:9-37.
- Matschiner, M., A. Böhne, F. Ronco, and W. Salzburger. 2020. The genomic timeline of cichlid fish diversification across continents. Nature Communications 11:5895.
- McGee, M. D., S. R. Borstein, J. I. Meier, D. A. Marques, S. Mwaiko, A. Taabu, M. A. Kishe, B. O'Meara, R. Bruggmann, L. Excoffier, and O. Seehausen. 2020. The ecological and genomic basis of explosive adaptive radiation. Nature 586:75-79.
- Meier, J. I., D. A. Marques, S. Mwaiko, C. E. Wagner, L. Excoffier, and O. Seehausen. 2017. Ancient hybridization fuels rapid cichlid fish adaptive radiations. Nature Communications 8:14363.
- Ronco, F., M. Matschiner, A. Böhne, A. Boila, H. H. Büscher, A. El Taher, A. Indermaur, M. Malinsky, V. Ricci, A. Kahman, S. Jentoft, and W. Salzburger. 2021. Drivers and dynamics of massive adaptive radiation in cichlid fishes. Nature 589:76-81.

- Seehausen, O. 1996. Lake Victoria rock cichlids, taxonomy, ecology and distribution. Verduijn Cichlids, Zevenhuizen, Netherlands.
- Seehausen, O., E. Lippitsch, N. Bouton, H. Zwennes. 1998. Mbipi, the rock-dwelling cichlids of Lake Victoria: description of three new genera and fifteen new species (Teleostei). Ichthyological Exploration of Freshwaters 9:129-228.
- Sparks, J. S. 2004. Molecular phylogeny and biogeography of the Malagasy and South Asian cichlids (Teleostei: Perciformes: Cichlidae). Molecular Phylogenetics and Evolution. 30:599–614.
- Sparks, J. S., and W. L. Smith. 2004. Phylogeny and biogeography of cichlid fishes (Teleostei: Perciformes: Cichlidae). Cladistics 20:501–517.
- Stager, J. C., and T. C. Johnson. 2008. The late Pleistocene desiccation of Lake Victoria and the origin of its endemic biota. Hydrobiologia 596:5-16.
- Verheyen, E., W. Salzburger, J. Snoeks, A. Meyer. 2003. Origin of the superflock of cichlid fishes from Lake Victoria, East Africa. Science 300:325-329.